An IMEX-RK scheme for capturing similarity solutions in the multidimensional Burgers' equation
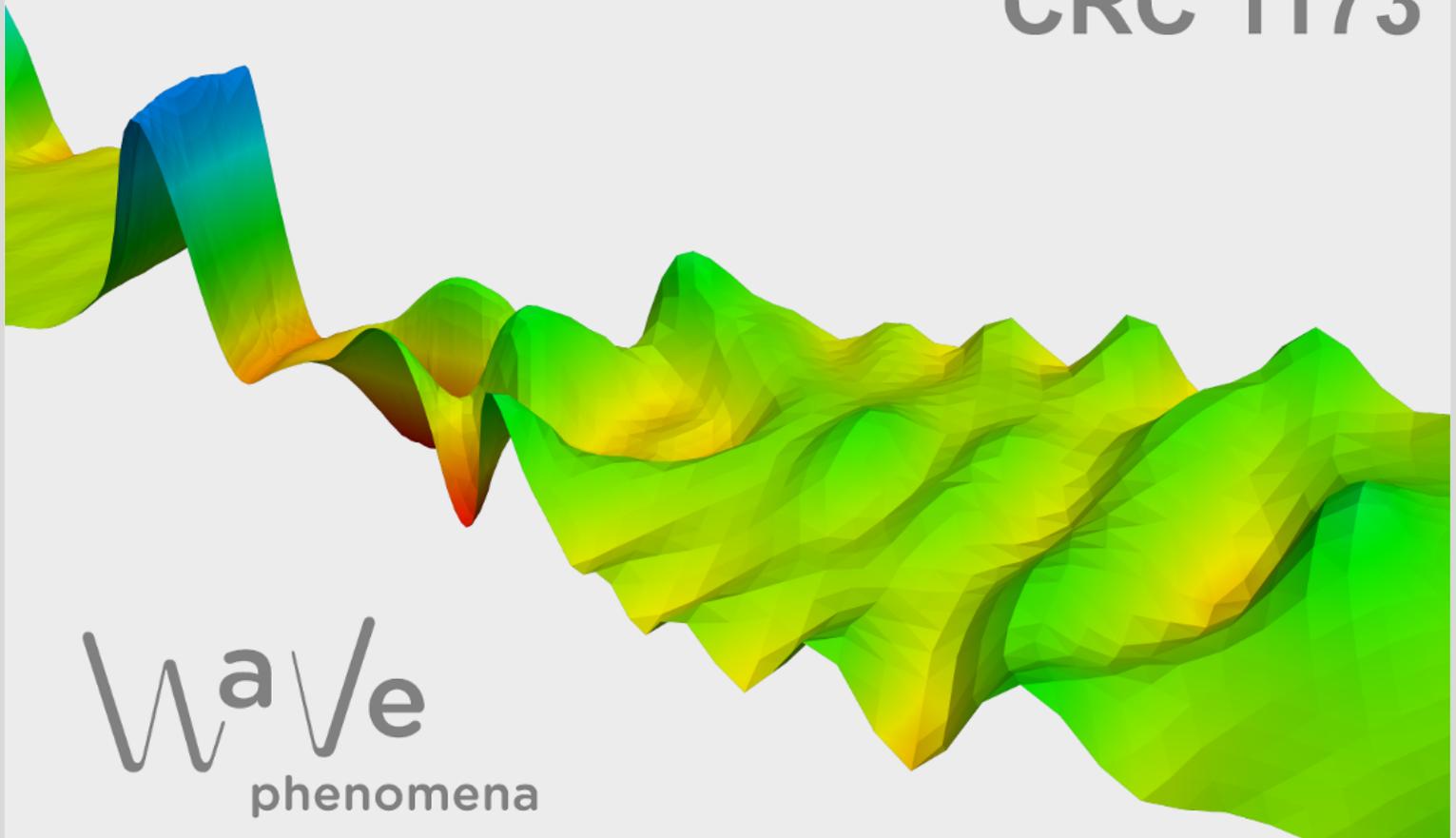
Jens Rottmann-Matthes

KARLSRUHE INSTITUTE OF TECHNOLOGY

CRC 1173

WaVe
phenomena

Zertifikat seit 2010
audit familiengerechte
hochschule

www.kit.edu

Participating universities

Universität Stuttgart

EBERHARD KARLS
UNIVERSITÄT
TÜBINGEN

Funded by

DFG

An IMEX-RK scheme for capturing similarity solutions in the multidimensional Burgers' equation

Jens Rottmann-Matthes[1]
Institute for Analysis
Karlsruhe Institute of Technology
76131 Karlsruhe
Germany

Date: December 13, 2016

Abstract. In this paper we introduce a new, simple and efficient numerical scheme for the implementation of the freezing method for capturing similarity solutions in partial differential equations. The scheme is based on an IMEX-Runge-Kutta approach for a method of lines (semi-)discretization of the freezing partial differential algebraic equation (PDAE). We prove second order convergence for the time discretization at smooth solutions in the ODE-sense and we present numerical experiments that show second order convergence for the full discretization of the PDAE.

As an example serves the multi-dimensional Burgers' equation. By considering very different sizes of viscosity, Burgers' equation can be considered as a prototypical example of general coupled hyperbolic-parabolic PDEs. Numerical experiments show that our method works perfectly well for all sizes of viscosity, suggesting that the scheme is indeed suitable for capturing similarity solutions in general hyperbolic-parabolic PDEs by direct forward simulation with the freezing method.

Key words. Similarity solutions, relative equilibria, Burgers' equation, freezing method, scaling symmetry, IMEX-Runge-Kutta, central scheme, hyperbolic-parabolic partial differential algebraic equations.
AMS subject classification. 65M20, 65M08, 35B06, 35B40, 35B30

1. Introduction

Many time-dependent partial differential equations from applications exhibit simple patterns. When these patterns are stable, solutions with sufficiently close initial data develop these patterns as as time increases. They often have important implications on the actual interpretation of the systems behavior. A very important and well-known example of a simple pattern are the traveling wave solutions which appear in the nerve-axon-equations of Hodgkin and Huxley. Here they model the transport of information along the axon of a nerve cell.

Traveling waves are one of the simplest examples of patterns which are relative equilibria. Relative equilibria are solutions to the evolution equation whose time evolution can be completely described by some curve in a symmetry group which acts on a fixed profile. In the case of a traveling wave, the profile is just the shape of the wave, the curve is a linear function into the group of the real numbers and the action is the shift of the profile. Of course, the slope of the curve is the velocity of the traveling wave. From an applications point of view, the velocity of the traveling pulse in the Hodgkin-Huxley system is of great relevance as it quantifies how fast information is passed on in this system.

The above example shows that one is often interested in relative equilibria of the underlying PDE problem and also in their specific constants of motion like their velocity. In a more mathematical way,

one has an evolution equation of the form

$$(1) \qquad u_t = F(u),$$

and a traveling wave is a solution $u(x,t)$ of (1) of the form $u(x,t) = \underline{u}(x - \underline{c}t)$, where $\underline{u}$ is a fixed profile and $\underline{c}$ is its velocity. When (1) is considered in a co-moving frame, i.e. with the new spatial coordinate $\xi = x - \underline{c}t$, the profile $\underline{u}$ becomes a steady state of the co-moving equation

$$(2) \qquad v_t = F(v) + \underline{c}v_\xi.$$

Similarly, there are evolution equations which exhibit rotating waves or spiral waves. In $d = 2$ spatial dimensions these are solutions of the form $u(x,t) = \underline{u}\left(\begin{pmatrix} \cos(\underline{c}t) & -\sin(\underline{c}t) \\ \sin(\underline{c}t) & \cos(\underline{c}t) \end{pmatrix} x\right)$. Considering the evolution equation (1) in a co-rotating frame, i.e. with the new spatial coordinates $\xi = \begin{pmatrix} \cos(\underline{c}t) & -\sin(\underline{c}t) \\ \sin(\underline{c}t) & \cos(\underline{c}t) \end{pmatrix} x$, the profile of a rotating wave becomes a steady state of the co-rotating equation

$$(3) \qquad v_t = F(v) + \underline{c}\xi_2 v_{\xi_1} - \underline{c}\xi_1 v_{\xi_2}.$$

Again, from an applications point of view, not only the profile $\underline{u}$ is of interest, but also the velocity $\underline{c}$ with which it rotates.

Typically, the velocities $\underline{c}$ of a traveling or rotating wave (or similar numbers for other relative equilibria) are not known in advance and thus the optimal co-moving coordinate frame, in which the solution becomes a steady state, cannot be used. A method, which calculates the solution to the Cauchy problem for (1) and in parallel a suitable reference frame is the freezing method, independently introduced in [5] and [15], see also [3]. A huge advantage of the method is that asymptotic stability with asymptotic phase of a traveling (or rotating) wave for the original system becomes asymptotic stability in the sense of Lyapunov of the waves profile and its velocity for the freezing system, see [18], [12], [13] and [3]. As such the method allows to approximate the profile and its constants of motion by a direct forward simulation. The method not only works for traveling, rotating or meandering waves but also for other relative equilibria and similarity solutions with a more complicated symmetry group, e.g. [3] or [14].

The idea of the method is to write the equation in new (time dependent) coordinates and to split the evolution of the solution into an evolution of the profile and an evolution in a symmetry group which brings the profile into the correct position via the group action. For example, in case of an $E(2)$ equivariance of the evolution equation ($E(2)$ is the Euclidean group of the plane), when we allow for rotation and translation in $\mathbb{R}^2$, this leads to

$$(4a) \qquad v_t = F(v) + \mu_1 \partial_{\xi_1} v + \mu_2 \partial_{\xi_2} v + \mu_3 \left(\xi_2 \partial_{\xi_1} v - \xi_1 \partial_{\xi_2} v\right).$$

In (4a) we have the new time dependent unknowns v and μ_1, μ_2, μ_3, where $\mu_j \in \mathbb{R}$. To cope with the additional degrees of freedom due to the μ_j, (4a) is supplemented by algebraic equations, so called phase conditions, which abstractly read

$$(4b) \qquad 0 = \Psi(v, \mu).$$

The complete system (4) is called the freezing system and the Cauchy problem for it can be implemented on a computer. Note that (4) in fact is a partial differential algebraic equation (PDAE).

In many cases the Cauchy problem for (4) can be solved by using standard software packages like COMSOL Multiphysics, see for example [3] or [4]. Nevertheless, in other cases these standard toolboxes may not work at all or may not give reliable results. For example this is the case for partly parabolic reaction-diffusion equations, i.e. reaction-diffusion equations in which not all component diffuse, as is the case in the important Hodgkin-Huxley equations. In this case the freezing method leads to a parabolic equation that is nonlinearly coupled to a hyperbolic equation with a time-varying principal part. Other examples which cannot easily be solved using standard packages include hyperbolic conservation laws or coupled hyperbolic-parabolic PDEs, which appear in many important applied problems.

In this article we present a new, simple and robust numerical discretization of the freezing PDAE which allows us to do long-term simulations of time-dependent PDEs and to capture similarity solutions, also for viscous and even inviscid conservation laws by the freezing method.

We derive our fully discrete scheme in two stages. First we do a spatial discretization of the freezing PDAE and obtain a method of lines (MOL) system. For the spatial discretization we employ a central scheme for hyperbolic conservation laws from Kurganov and Tadmor [10]. Namely, we adapt the semi-discrete scheme derived in [10] to the case, when the flux may depend also on the spatial variable. This yields a second order semi-discrete central scheme. It has the important property that it does not require information of the local wave structure besides an upper bound on the local wave speed. In particular, no solutions to Riemann problems are needed.

The resulting MOL system is a huge ordinary differential algebraic equation (ODAE) system, which has parts with very properties. On the one hand, parabolic parts lead for fine spatial discretizations to very stiff parts in the equation, for which one should employ implicit time-marching schemes. On the other hand, a hyperbolic term leads to a medium stiffness but becomes highly nonlinear due to the spatial discretization, so an explicit time-marching scheme is preferable. To couple these conflicting requirements, we use an implicit-explicit (IMEX) Runge-Kutta scheme for the time discretization. Such schemes were considered in [1], but here we will apply them to DAE problems.

As an example we consider Burgers' equation,

$$(5) \qquad u_t + \left(\tfrac{1}{2}u^2\right)_x = \nu u_{xx}, \quad x \in \mathbb{R},$$

which was originally introduce by J.M. Burgers (e.g. [6]) as a mathematical model of turbulence. We also consider the multidimensional generalizations of (5)

$$(6) \qquad u_t + \tfrac{1}{p}\operatorname{div}(a|u|^p) = \nu\Delta u, \quad x \in \mathbb{R}^d,$$

where $a \in \mathbb{R}^d \setminus \{0\}$ and $p > 1$ are fixed. Equation (5) and its generalization to d dimensions are among the simplest truly nonlinear partial differential equations and, moreover, in the inviscid ($\nu = 0$) case they develop shock solutions. As such they are often used as test problems for shock capturing schemes, e.g. [9]. But they are also of interest from a physical point of view as they are special cases of *the* "multidimensional Burgers' equation"

$$(7) \qquad \partial_t \vec{u} + (\vec{u} \cdot \nabla)\vec{u} = \nu\,\Delta\,\vec{u},$$

which has applications in different areas of physics, e.g. see the review [2].

There are mainly three reasons for us, why we choose Burgers' equation as an example. First of all, it is a very simple (scalar) nonlinear equation. But despite its simplicity, it suits as an example for which the hyperbolic part dominates by choosing $0 < \nu << 1$ and it also suits as an example for which the parabolic part dominates by choosing $\nu >> 0$. And third, as we will see below, the new terms, introduced by the freezing method, have properties very similar to the terms appearing in the method of freezing for rotating waves.

The plan of the paper is as follows. In Section 2 we derive the continuous freezing method for Burgers' equation and present the analytic background In Section 3 we explain the spatial discretization of the freezing PDAE and obtain the method of lines ordinary DAE approximation. In the subsequent step in Section 4 we then do the time-discretization of the DAE with our IMEX Runge-Kutta scheme and show that it is a second order method for the DAE (with respect to the differential variables). In the final Section 5 we present several numerical results which show that our method and its numerical discretization are suitable for freezing patterns in equations for which the parabolic part dominates and also for equations for which the hyperbolic part dominates. Because of this we expect our method to be well suited also for capturing traveling or rotating waves in hyperbolic-parabolic coupled problems.

2. The Continuous Freezing System

In this section we briefly review the results from [14] and explain the freezing system for Burgers' equation (6). For the benefit of the reader, though, we present a simplified and direct derivation without using the abstract language and theory of Lie groups and Lie algebras. We refer to [14] for the abstract approach.

2.1. **The Co-Moved System.** To formally derive the freezing system, we assume that the solution u of the Cauchy problem for (6),

$$
(8) \qquad \begin{cases} u_t = \nu \, \Delta \, u - \dfrac{1}{p} \operatorname{div}_x \big(a|u|^p\big) =: F(u), \\[2mm] u(0) = u_0, \end{cases}
$$

is of the form

$$
(9) \qquad u(x,t) = \frac{1}{\alpha\big(\tau(t)\big)} \, v\left(\frac{x - b\big(\tau(t)\big)}{\alpha\big(\tau(t)\big)^{p-1}}, \tau(t)\right),
$$

where $v : \mathbb{R}^d \times \mathbb{R} \to \mathbb{R}$, $b = (b_1, \dots, b_d)^\top : \mathbb{R} \to \mathbb{R}^d$, $\alpha : \mathbb{R} \to (0, \infty)$, and $\tau : [0, \infty) \to [0, \infty)$ are smooth functions and $\dot{\tau}(t) > 0$ for all $t \in [0, \infty)$.

Remarks.   (i) One can interpret the function τ as a transformation of the time t to a new time τ, the action of the scalar function α on the function v can be understood as a scaling of the function and the space. Finally, we interpret the meaning of b as a spatial shift.

(ii) Note that in [14] we also allow for a spatial rotation. We actually do not use the rotational symmetry here because it does not appear in one and two spatial dimensions. Moreover, the symmetries we consider here are also present in the multi-dimensional Burgers' system (7), whereas the rotational symmetry is not.

A simple calculation shows

$$
(10) \qquad F(u)(x,t) = \frac{1}{\alpha^{2p-1}} F(v)\,(\xi, \tau),
$$

where $\xi = \frac{x-b}{\alpha^{p-1}}$ denotes new spatial coordinates. Moreover, from (9), we obtain with the chain rule

$$
(11) \qquad \begin{aligned} \frac{\partial}{\partial t} u(x,t) &= \frac{d}{dt}\left(\frac{1}{\alpha(\tau(t))}\, v\left(\frac{x-b(\tau(t))}{\alpha(\tau(t))^{p-1}}, \tau(t)\right)\right) \\[2mm] &= -\frac{\alpha'(\tau)}{\alpha^2(\tau)}\dot{\tau}v(\xi,\tau) - (p-1)\frac{\alpha'(\tau)}{\alpha^2}\xi^\top \nabla_\xi v(\xi,\tau)\dot{\tau} - \frac{b'(\tau)^\top}{\alpha(\tau)^p}\nabla_\xi v(\xi,\tau)\dot{\tau} + \frac{1}{\alpha(\tau)}v_\tau(\xi,\tau)\dot{\tau}. \end{aligned}
$$

By setting

$$
(12) \qquad \mu_1(\tau) = \frac{\alpha'(\tau)}{\alpha(\tau)} \in \mathbb{R} \quad \text{and} \quad \mu_{i+1}(\tau) = \frac{b'_i(\tau)}{\alpha(\tau)^{p-1}} \in \mathbb{R}, i = 1, \dots, d,
$$

$$
(13) \qquad \phi_1(\xi, v) = -(p-1)\operatorname{div}_\xi(\xi v) - (1 - d(p-1))v \quad \text{and} \quad \phi_2(\xi, v) = -\nabla_\xi v = -\left(\frac{\partial}{\partial \xi_j} v\right)_{j=1}^d,
$$

we can write (11) as

$$
(14) \qquad \frac{\partial}{\partial t} u(x,t) = \frac{1}{\alpha(\tau)}\Big(\mu_1(\tau)\phi_1(\xi, v) + \mu_{(2:d+1)}(\tau)\phi_2(\xi, v) + v_\tau\Big)\dot{\tau},
$$

where $\mu_{(2:d+1)} = (\mu_2, \dots, \mu_{d+1})$. Because u solves (8), we obtain from (10) and (14) under the assumption that τ satisfies

$$
(15) \qquad \dot{\tau} = \alpha(\tau)^{2-2p}.
$$

in the new ξ, τ, v coordinates for v the equation

(16) $$v_\tau = F(v) - \mu_1 \phi_1(\xi, v) - \mu_{(2:d+1)} \phi_2(\xi, v).$$

The key observation for the freezing method is Theorem 4.2 from [14], which relates the solution of the original Cauchy problem (8) to the solution of the Cauchy problem for (16) in the new (ξ, τ) coordinates. Using the spaces $X = L^2(\mathbb{R}^d)$ and $Y_1 = \left\{ v \in H^2(\mathbb{R}^d) : \xi^\top \nabla_\xi v \in L^2(\mathbb{R}^d) \right\}$ the result from [14] can be rephrased as follows:

Theorem 2.1. *A function* $u \in \mathcal{C}([0, T); Y_1) \cap \mathcal{C}^1([0, T); X)$ *solves* (8) *if and only if the functions* $v \in \mathcal{C}([0, \widehat{T}); Y_1) \cap \mathcal{C}^1([0, \widehat{T}); X)$, $\mu_i \in \mathcal{C}([0, \widehat{T}); \mathbb{R})$, $i = 1, \ldots, d+1$, $\alpha \in \mathcal{C}^1([0, \widehat{T}); (0, \infty))$, $b \in \mathcal{C}^1([0, \widehat{T}); \mathbb{R}^d)$, *and* $\tau \in \mathcal{C}^1([0, T); [0, \widehat{T}))$ *solve the system*

(17)
$$\begin{aligned}
v_\tau &= F(v) - \mu_1 \phi_1(\xi, v) - \mu_{(2:d+1)} \phi_2(\xi, v), & v(0) &= u_0, \\
\alpha_\tau &= \mu_1 \, \alpha, & \alpha(0) &= 1, \\
b_\tau &= \alpha^{p-1} \mu_{(2:d+1)}^\top, & b(0) &= 0, \\
\frac{\partial}{\partial t} \tau &= \alpha(\tau)^{2-2p}, & \tau(0) &= 0,
\end{aligned}$$

and u *and* v, α, b, τ *are related by* (9).

2.2. The Freezing System. To cope with the $d+1$ additional degrees of freedom, due to $\mu_1, \ldots, \mu_{d+1}$, we complement (17) with $d + 1$ algebraic equations, so called phase conditions, see [5].

Type 1: Orthogonal phase condition. We require that v, and $\mu_1, \ldots, \mu_{d+1}$ which solve (16), are chosen such that at each time instance $\|v_\tau\|_{L^2}^2$ is minimized with respect to $\mu_1, \ldots, \mu_{d+1}$. Therefore, we have

$$0 = \frac{1}{2} \frac{d}{d\mu} \big\| F(v) - \mu_1 \phi_1(\xi, v) - \mu_{(2:d+1)} \phi_2(\xi, v) \big\|_{L^2}^2$$

which is equivalent to

(18)
$$\begin{cases}
0 = \Big\langle \phi_1(\xi, v), F(v) - \mu_1 \phi_1(\xi, v) - \mu_{(2:d+1)} \phi_2(\xi, v) \Big\rangle_{L^2}, \\
0 = \Big\langle \dfrac{\partial}{\partial \xi_j} v, F(v) - \mu_1 \phi_1(\xi, v) - \mu_{(2:d+1)} \phi_2(\xi, v) \Big\rangle_{L^2}, \; j = 1, \ldots, d,
\end{cases}$$

where ϕ_1 and ϕ_2 are given in (13). We abbreviate (18) as $0 = \Psi^{\mathrm{orth}}(v, \mu)$.

Type 2: Fixed phase condition. The idea of the fixed phase condition is, to require that the v-component of the solution always lies in a fixed, $d + 1$-co-dimensional hyperplane, which is given as the level set of a fixed, linear mapping. Here we assume that a "suitable" reference function $\widehat{u}$ is given and the v-component of the solution always satisfies

(19)
$$\begin{cases}
0 = \Big\langle \phi_1(\xi, \widehat{u}), \widehat{u} - v \Big\rangle_{L^2}, \\
0 = \Big\langle \dfrac{\partial}{\partial \xi_j} \widehat{u}, \widehat{u} - v \Big\rangle_{L^2}, \; j = 1, \ldots, d,
\end{cases}$$

where ϕ_1 and ϕ_2 are given in (13). We abbreviate (19) as $0 = \Psi^{\mathrm{fix}}(v)$.

We augment system (17) with one of the phase conditions (18) or (19) and obtain

(20a) $$v_\tau = F(v) - \mu_1 \phi_1(\xi, v) - \mu_{(2:d+1)} \phi_2(\xi, v), \qquad v(0) = u_0,$$

(20b) $$0 = \Psi(v, \mu),$$

(20c) $$\alpha_\tau = \mu_1 \alpha, \; b_\tau = \alpha^{p-1} \mu_{(2:d+1)}^\top, \qquad\qquad \alpha(0) = 1 \in \mathbb{R}, \; b(0) = 0 \in \mathbb{R}^d,$$

(20d) $$\frac{d}{d\tau} t = \alpha(\tau)^{2p-2}, \qquad\qquad t(0) = 0,$$

where $\Psi(v, \mu)$ is either Ψ^{orth} from (18) or Ψ^{fix} from (19).

Remark 2.2. (i) Observe that (20) consists of the PDE (20a), coupled to a system of ordinary differential equations (20c) and (20d), and coupled to a system of algebraic equations (20b). Moreover, in (20a) the hyperbolic part dominates for $0 < \nu \ll 1$ and the parabolic part dominates for $\nu \gg 0$. Finally, note that the ordinary differential equations (20c) and (20d) decouple from (20a) and (20b) can be solved in a post-processing step.

  (ii) Note that the ϕ_1-term in (13) resembles the generator of rotation, cf. (4a).

  (iii) Under suitable assumptions on the solution and the reference function, the system (20a), (20b) is a PDAE of "time-index" 1 in the case $\Psi = \Psi^{\mathrm{orth}}$ and of "time-index" 2 in the case $\Psi = \Psi^{\mathrm{fix}}$, where the index is understood as differentiation index, see [11].

3. Implementation of the Numerical Freezing Method I: Spatial Discretization

In this section we derive a spatial semi-discretization (Method of Lines system) of the freezing partial differential algebraic evolution equation system (20). First we separately consider the PDE-part (20a) of the equation on the full domain. Afterwards we consider the case of a bounded domain with artificial no-flux boundary conditions. Finally, we consider the spatial discretization of the (low-dimensional) remaining equations (20b)–(20d).

3.1. Spatial Semi-Discretization of the PDE-Part.

Recall from (13), that $\mu_1 \phi_1(\xi, v)$ is of the form

$$\mu_1 \phi_1(\xi, v) = \mu_1 \sum_{j=1}^{d} \frac{d}{d\xi_j} f_{1,j}(\xi, v) - \mu_1 f_{1,0}(v),$$

where $f_{1,0}(v) = \big(1 - d(p-1)\big)v$ and $f_{1,j}(\xi, v) = -(p-1)\xi_j v$. Note that $\frac{d}{d\xi_j} f(\xi, v) = \frac{\partial}{\partial \xi_j} f + \frac{\partial}{\partial v} f \frac{\partial}{\partial \xi_j} v$. Similarly, the term $\mu_{(2:d+1)} \phi_2(\xi, v)$ can be written as

$$\mu_{(2:d+1)} \phi_2(\xi, v) = -\sum_{i=1}^{d} \mu_{1+i} \frac{\partial}{\partial \xi_i} v = \sum_{i=1}^{d} \mu_{1+i} \sum_{j=1}^{d} \frac{d}{d\xi_j} f_{1+i,j}(\xi, v),$$

where $f_{1+i,j}(\xi, v) = -v$ if $i = j$ and $f_{1+i,j}(\xi, v) = 0$ if $i \neq 0$, $i, j = 1, \dots, d$. Furthermore, by also setting $f_{0,j}(v) = \frac{1}{p} a_j |v|^p$, equation (20a) can be recast as

$$(21) \qquad v_\tau + \sum_{i=1}^{d+1} \mu_i \Big[\sum_{j=1}^{d} \frac{d}{d\xi_j} f_{i,j}(\xi, v) \Big] + \sum_{j=1}^{d} \frac{d}{d\xi_j} f_{0,j}(v) = \sum_{j=1}^{d} \frac{d}{d\xi_j} Q_j \big(\tfrac{\partial}{\partial \xi_j} v \big) + \mu_1 f_{1,0}(v).$$

For the spatial semi-discretization we adapt the 2nd order semi-discrete central scheme for hyperbolic conservation laws from [10] to our situation. The details of the adaptation to space dependent hyperbolic conservation laws of the form

$$(22) \qquad v_\tau + \sum_{j=1}^{d} \frac{d}{d\xi_j} f_j(\xi, v) = 0$$

is presented in Appendix A. As is noted in [10, § 4], diffusive flux terms and zero order terms, which appear in (21), can easily be appended to the semi-discretization of (22) by simple second order finite difference approximations.

For the actual discretization we choose a uniform spatial grid in each coordinate direction

$$\xi_{k-\frac{1}{2}}^{j} = (k - \frac{1}{2}) \Delta \xi_j, \ k \in \mathbb{Z}, \ j = 1, \dots, d,$$

and obtain the rectangular cells (finite volumes) $C_{\mathbf{k}} := C_{k_1,\ldots,k_d} := \bigtimes_{j=1}^d (\xi_{k_j-\frac{1}{2}}^j, \xi_{k_j+\frac{1}{2}}^j) \subset \mathbb{R}^d$, with centers $\xi_{\mathbf{k}} := (\xi_{k_1}^1, \ldots, \xi_{k_d}^d) \in \mathbb{R}^d$, where $\mathbf{k} = (k_1, \ldots, k_d) \in \mathbb{K}$ with index set $\mathbb{K} = \mathbb{Z}^d$. In the following we interpret for each $\mathbf{k} \in \mathbb{K}$, $v_{\mathbf{k}}(\tau)$ as an approximation of the cell-average of v in the cell $C_{\mathbf{k}}$ at time τ,

$$v_{\mathbf{k}}(\tau) \approx \frac{1}{\text{vol}(C_{\mathbf{k}})} \int_{C_{\mathbf{k}}} v(\xi, \tau)\, d\xi, \quad \text{vol}(C_{\mathbf{k}}) = \prod_{j=1}^d \Delta\xi_j.$$

Then the method-of-lines system for (21) is given by

$$(23) \quad v_{\mathbf{k}}' = -\sum_{j=1}^d \frac{H_{\mathbf{k}^j+\frac{1}{2}}^{0,j} - H_{\mathbf{k}^j-\frac{1}{2}}^{0,j}}{\Delta\xi_j} - \sum_{i=1}^{d+1} \mu_i \sum_{j=1}^d \frac{H_{\mathbf{k}^j+\frac{1}{2}}^{i,j} - H_{\mathbf{k}^j-\frac{1}{2}}^{i,j}}{\Delta\xi_j} + \mu_1 f_{1,0}(v_{\mathbf{k}})$$

$$+ \sum_{j=1}^d \frac{P_{\mathbf{k}^j+\frac{1}{2}}^j - P_{\mathbf{k}^j-\frac{1}{2}}^j}{\Delta\xi_j} =: F_{\mathbf{k}}(v_{\mathbb{Z}^d}, \mu), \quad \mathbf{k} \in \mathbb{K}.$$

In (23) we use the following notations and abbreviations:
For $\mathbf{k} = (k_1, \ldots, k_d) \in \mathbb{K}$, we denote $\mathbf{k}^j \pm \frac{1}{2} := (k_1, \ldots, k_{j-1}, k_j \pm \frac{1}{2}, k_{j+1}, \ldots, k_d)$. Then $H_{\mathbf{k}^j\pm\frac{1}{2}}^{i,j}(t)$ is an approximation of the *"hyperbolic flux"* through the boundary face

$$(\xi_{k_1-\frac{1}{2}}^1, \xi_{k_1+\frac{1}{2}}^1) \times \cdots \times \{\xi_{k_j\pm\frac{1}{2}}^j\} \times \cdots \times (\xi_{k_d-\frac{1}{2}}^d, \xi_{k_d+\frac{1}{2}}^d) =: \partial C_{\mathbf{k}^j\pm\frac{1}{2}}$$

of $C_{\mathbf{k}}$ due to the flux function $f_{i,j}$, $i = 0, \ldots, d+1$, $j = 1, \ldots, d$. Moreover, we add the regularizing part of the KT-scheme completely to the $H^{0,j}$-terms. Namely the term $\frac{a}{2\Delta\xi}(u_{k-\frac{1}{2}}^- - u_{k-\frac{1}{2}}^+ - u_{k+\frac{1}{2}}^- + u_{k+\frac{1}{2}}^+)$ from (79) is added to the discretization of $\frac{d}{d\xi} f_{0,1}(v)$ in the 1-dimensional case. In the 2-dimensional case the term $\frac{a}{2\Delta\xi}(u_{k_1-\frac{1}{2},k_2}^- - u_{k_1-\frac{1}{2},k_2}^+ - u_{k_1+\frac{1}{2},k_2}^- + u_{k_1+\frac{1}{2},k_2}^+)$ from (81) is added to the discretization of $\frac{d}{d\xi_1} f_{0,1}(v)$ and the term $\frac{a}{2\Delta\eta}(u_{k_1,k_2-\frac{1}{2}}^- - u_{k_1,k_2-\frac{1}{2}}^+ - u_{k_1,k_2+\frac{1}{2}}^- + u_{k_1,k_2+\frac{1}{2}}^+)$ from (81) is added to the discretization of $\frac{d}{d\xi_2} f_{0,2}(v)$. Hence the $H^{i,j}$, $i = 0, \ldots, d+1$, $j = 1, \ldots, d$ take the form

$$(24) \qquad H_{\mathbf{k}^j\pm\frac{1}{2}}^{i,j}(t) = \frac{f_{i,j}(\xi_{\mathbf{k}^j\pm\frac{1}{2}}, v_{\mathbf{k}^j\pm\frac{1}{2}}^+) + f_{i,j}(\xi_{\mathbf{k}^j\pm\frac{1}{2}}, v_{\mathbf{k}^j\pm\frac{1}{2}}^-)}{2} - \delta_{i,0}\mathbf{a}(v_{\mathbf{k}^j\pm\frac{1}{2}}^+ - v_{\mathbf{k}^j\pm\frac{1}{2}}^-).$$

In (24) the point of evaluation is

$$(25) \qquad \xi_{\mathbf{k}^j\pm\frac{1}{2}} = (\xi_{k_1}, \ldots, \xi_{k_d}) \pm \tfrac{1}{2}\mathrm{e}_j\Delta\xi_j \in \partial C_{\mathbf{k}},$$

and $v_{\mathbf{k}^j+\frac{1}{2}}^+$, $v_{\mathbf{k}^j+\frac{1}{2}}^-$ denote the limits "from above" and "from below" at the boundary face $\partial C_{\mathbf{k}^j+\frac{1}{2}}$ of the piecewise linear minmod-reconstruction $\hat{v}$ of $(v_{\mathbf{k}})_{\mathbf{k}\in\mathbb{Z}^d}$, explained in the Appendix A, i.e.

$$(26) \qquad v_{\mathbf{k}^j+\frac{1}{2}}^+ = \lim_{h\searrow\frac{1}{2}} \hat{v}(x_{\mathbf{k}} + h\Delta x_j\mathrm{e}_j), \ v_{\mathbf{k}^j+\frac{1}{2}}^- = \lim_{h\nearrow\frac{1}{2}} \hat{v}(x_{\mathbf{k}} + h\Delta x_j\mathrm{e}_j).$$

For explicit formulas of $v_{\mathbf{k}^j+\frac{1}{2}}^\pm$ in the 1d and 2d case see (80) and (82), respectively.

Moreover, the value $\mathbf{a}$, appearing in $H_{\mathbf{k}^j\pm\frac{1}{2}}^{0,j}$, denotes an upper bound for the maximal wave speeds of the hyperbolic terms. The choice of the value $\mathbf{a}$ is only formal at the moment, because such a number does not exist in case of a non-trivial scaling. But note that for the actual numerical computations performed in Section 5, we have to restrict to a bounded domain and on bounded domains the number $\mathbf{a}$ is always finite.

The term $f_{1,0}(v_{\mathbf{k}})$ in (23) is an approximation of the average source term $f_{1,0}(v)$ on the cell $C_{\mathbf{k}}$.

Finally, $P^j_{\mathbf{k}^j+\frac{1}{2}}$, $\mathbf{k} = (k_1, \ldots, k_d) \in \mathbb{K}$, denotes an approximation of the "*diffusion flux*" through the boundary face $\partial C_{\mathbf{k}^j+\frac{1}{2}}$, due to the flux function $Q_j(\frac{\partial}{\partial \xi_j} v)$. This is simply approximated by

$$(27) \qquad P^j_{\mathbf{k}^j+\frac{1}{2}} = Q_j\left(\frac{v_{\mathbf{k}+\mathbf{e}_j} - v_{\mathbf{k}}}{\Delta \xi_j}\right).$$

There is no difficulty in generalizing to diffusion fluxes of the form $Q_j(v, \frac{\partial}{\partial \xi_j} v)$, see [10, § 4].

Remark. (i) The upper index j in (23)–(27), corresponds to the jth coordinate direction, i.e.

$$-\frac{H^{0,j}_{\mathbf{k}^j+\frac{1}{2}} - H^{0,j}_{\mathbf{k}^j-\frac{1}{2}}}{\Delta \xi_j} - \sum_{i=1}^{d+1} \mu_i \frac{H^{i,j}_{\mathbf{k}^j+\frac{1}{2}} - H^{i,j}_{\mathbf{k}^j-\frac{1}{2}}}{\Delta \xi_j} + \frac{P^j_{\mathbf{k}^j+\frac{1}{2}} - P^j_{\mathbf{k}^j-\frac{1}{2}}}{\Delta \xi_j}$$

is the numerical flux in the jth direction and H stands for the hyperbolic flux and P for the dissipative flux.

(ii) In the derivation of (23) we make essential use of the the property that the method (79) and its multi-dimensional variants (e.g. (81)) depend linearly on the flux function, see Remark A.1.

3.2. Artificial No-Flux Boundary Conditions.

Equation (23) is an infinite dimensional system of ordinary differential equations and hence not implementable on a computer. Therefore, we restrict (20) to a bounded domain. For simplicity we only consider rectangular domains of the form

$$(28) \qquad \Omega = \left\{\xi = (\xi_1, \ldots, \xi_d) \in \mathbb{R}^d : R_j^- \leq \xi_j \leq R_j^+, j = 1, \ldots, d\right\}$$

with $R_j^- < R_j^+ \in \mathbb{R}$. For the PDE-part (20a) we then impose no-flux boundary conditions on $\partial \Omega$. We perform the method-of-lines approach as presented in the previous Subsection 3.1. For this we assume that the grid in the jth coordinate direction, $j = 1, \ldots, d$, is given by

$$\xi^j_{k_j - \frac{1}{2}} = R_j^- + k_j \Delta \xi_j, \; k_j = 0, \ldots, N_j + 1, \text{ with } \xi^j_{N_j+\frac{1}{2}} = R_j^+.$$

Again $\mathbb{K} := \{\mathbf{k} = (k_1, \ldots, k_d) \in \mathbb{Z}^d : 0 \leq k_j \leq N_j + 1, j = 1, \ldots, d\}$ denotes the index set and the cells (finite volumes) are

$$C_{\mathbf{k}} := C_{k_1, \ldots, k_d} := \times_{j=1}^d (\xi^j_{k_j-\frac{1}{2}}, \xi^j_{k_j+\frac{1}{2}}), \quad \mathbf{k} \in \mathbb{K}.$$

The cell $C_{\mathbf{k}}$ has the center $\xi_{\mathbf{k}} = (\xi^1_{k_1}, \ldots, \xi^d_{k_d})$.

For the resulting discretization of (20a) on Ω, which is of the form (23), it is easy to implement no-flux boundary conditions by imposing for $i = 0, \ldots, d + 1$, $j = 1, \ldots, d$

$$(29) \qquad H^{i,j}_{\mathbf{k}^j\pm\frac{1}{2}} = 0 \text{ and } P^j_{\mathbf{k}^j\pm\frac{1}{2}} = 0 \text{ if } \xi_{\mathbf{k}^j\pm\frac{1}{2}} \in \partial\Omega.$$

Moreover, an explicit upper bound $\mathbf{a}$ of the local wave speeds in (24) is

$$(30) \qquad \mathbf{a} = \max_{\xi\in\Omega} \max_j \left[\sum_{i=1}^{\dim \mathfrak{g}} \mu_i \frac{\partial}{\partial v} f_{i,j}(\xi, v) + \frac{\partial}{\partial v} f_{0,j}(v)\right].$$

Thus we obtain a method-of-lines approximation of (20a) on Ω subject to (artificial) no-flux boundary conditions on $\partial\Omega$ by the formula (23) for $\mathbf{k} \in \mathbb{K}$ with (24), (25), (26), (27), (29), and (30).

3.3. Spatial Semi-Discretization of ODE- and Algebraic-Part.

Because (20c) and (20d) are already (low-dimensional) ordinary differential equations and do not explicitly depend on the values of the function v, nothing has to be done for their spatial discretizations. Thus it remains to discretize (20b), the phase conditions. In this article we assume that they are given by one of the formulas (18)

or (19). These integral conditions can easily be discretized by using average values of the function on a cell. Namely, we approximate (18) by the system

$$
(31) \qquad 0 = \sum_{\mathbf{k} \in \mathbb{K}} \mathrm{vol}(C_{\mathbf{k}}) \bigg[\bigg(-\sum_{j=1}^{d} \frac{H^{i,j}_{\mathbf{k}^j + \frac{1}{2}} - H^{i,j}_{\mathbf{k}^j - \frac{1}{2}}}{\Delta \xi_j} + \delta_{i,1} f_{1,0}(v_{\mathbf{k}}) \bigg) \cdot F_{\mathbf{k}}(v_{\mathbb{K}}, \mu) \bigg], \ i = 1, \dots, d+1
$$

of $d+1$ algebraic equations. Similarly, we approximate (19) by

$$
(32) \quad 0 = \sum_{\mathbf{k} \in \mathbb{K}} \mathrm{vol}(C_{\mathbf{k}}) \bigg[\bigg(-\sum_{j=1}^{d} \frac{H^{i,j}_{\mathbf{k}^j + \frac{1}{2}}(\widehat{u}_{\mathbb{K}}) - H^{i,j}_{\mathbf{k}^j - \frac{1}{2}}(\widehat{u}_{\mathbb{K}})}{\Delta \xi_j} + \delta_{i,1} f_{1,0}(\widehat{u}_{\mathbf{k}}) \bigg) \cdot \big(v_{\mathbf{k}} - \widehat{u}_{\mathbf{k}} \big) \bigg], \ i = 1, \dots, d+1,
$$

where $\widehat{u}_{\mathbf{k}}$ is an approximation of the average value of the reference function $\widehat{u}$ in the cell $C_{\mathbf{k}}$, $\widehat{u}_{\mathbb{K}} = (\widehat{u}_{\mathbf{k}})_{\mathbf{k} \in \mathbb{K}}$, and $H^{i,j}_{\mathbf{k}^j \pm \frac{1}{2}}(\widehat{u}_{\mathbb{K}})$ is given by (24) with v replaced by $(\widehat{u}_{\mathbf{k}})_{\mathbf{k} \in \mathbb{K}}$.

Remark 3.1. The evaluation of the phase conditions (31) and (32) is cheap and easily obtained. Because the terms $H^{i,j}_{\mathbf{k}^j \pm \frac{1}{2}}$ and $f_{1,0}(v_{\mathbf{k}})$ in (31) are anyway needed for the evaluation of $F_{\mathbf{k}}$.

Similarly, for the discretization of (32) one only needs to calculate the $H^{i,j}_{\mathbf{k}^j \pm \frac{1}{2}}(\widehat{u})$ once and has to remember the result of this calculation. In the special case when one chooses some previous value $v_{\mathbb{K}}$ as reference solution, the value of $H^{i,j}_{\mathbf{k}^j \pm \frac{1}{2}}(\widehat{u})$ is even already known.

3.4. **The Final Method of Lines System.** Recollecting the above discussion, the method of lines approximation of the freezing PDAE (20) takes the final form

$$
(33a) \qquad v'_{\mathbf{k}} = -H^0_{\mathbf{k}}(v_{\mathbb{K}}) - H^1_{\mathbf{k}}(v_{\mathbb{K}})\mu + P_{\mathbf{k}}(v_{\mathbb{K}}) =: F_{\mathbf{k}}(v_{\mathbb{K}}, \mu), \quad \mathbf{k} \in \mathbb{K},
$$

$$
(33b) \qquad 0 = \begin{cases} H^1(v_{\mathbb{K}})^{\top} F(v_{\mathbb{K}}, \mu), & \text{orthogonal Phase,} \\ H^1(\widehat{u}_{\mathbb{K}})^{\top}(v_{\mathbb{K}} - \widehat{u}_{\mathbb{K}}), & \text{fixed Phase,} \end{cases}
$$

$$
(33c) \qquad g' = r_{\mathrm{alg}}(g, \mu),
$$

$$
(33d) \qquad t' = r_{\mathrm{time}}(g),
$$

with initial data $v_{\mathbf{k}} \approx \frac{1}{\mathrm{vol}(C_{\mathbf{k}})} \int_{C_{\mathbf{k}}} u_0(\xi) \, d\xi$ for $\mathbf{k} \in \mathbb{K}$, $g(0) = \big(\alpha(0), b(0)^{\top}\big)^{\top} = (1, 0, \dots, 0)^{\top}$, and $t(0) = 0$. In (33) we use the abbreviations $\mu = (\mu_1, \dots, \mu_{d+1})^{\top} \in \mathbb{R}^{d+1}$ and

$$
H^0_{\mathbf{k}}(v_{\mathbb{K}}) = \sum_{j=1}^{d} \frac{H^{0,j}_{\mathbf{k}^j + \frac{1}{2}} - H^{0,j}_{\mathbf{k}^j - \frac{1}{2}}}{\Delta \xi_j}, \qquad\qquad\qquad\qquad H^0(v_{\mathbb{K}}) = \big(H^0_{\mathbf{k}}(v_{\mathbb{K}}) \big)_{\mathbf{k} \in \mathbb{K}},
$$

$$
H^1_{\mathbf{k}}(v_{\mathbb{K}}) = \bigg(-f_{1,0}(v_{\mathbf{k}}) + \sum_{j=1}^{d} \frac{H^{1,j}_{\mathbf{k}^j + \frac{1}{2}} - H^{1,j}_{\mathbf{k}^j - \frac{1}{2}}}{\Delta \xi_j}, \dots, \sum_{j=1}^{d} \frac{H^{d+1,j}_{\mathbf{k}^j + \frac{1}{2}} - H^{d+1,j}_{\mathbf{k}^j - \frac{1}{2}}}{\Delta \xi_j} \bigg), \quad H^1(v_{\mathbb{K}}) = \big(H^1_{\mathbf{k}}(v_{\mathbb{K}}) \big)_{\mathbf{k} \in \mathbb{K}},
$$

$$
P_{\mathbf{k}}(v_{\mathbb{K}}) = \sum_{j=1}^{d} \frac{P^{j}_{\mathbf{k}^j + \frac{1}{2}} - P^{j}_{\mathbf{k}^j - \frac{1}{2}}}{\Delta \xi_j}, \qquad\qquad\qquad\qquad P(v_{\mathbb{K}}) = \big(P_{\mathbf{k}}(v_{\mathbb{K}}) \big)_{\mathbf{k} \in \mathbb{K}},
$$

$$
F(v_{\mathbb{K}}, \mu) = \big(F_{\mathbf{k}}(v_{\mathbb{K}}, \mu) \big)_{\mathbf{k} \in \mathbb{K}},
$$

$$
g = \begin{pmatrix} \alpha \\ b \end{pmatrix}, \quad r_{\mathrm{alg}}(g, \mu) = \begin{pmatrix} g_1 \mu_1 \\ g_1^{p-1} \mu_{(2:d+1)}^{\top} \end{pmatrix} = \begin{pmatrix} \alpha \mu_1 \\ \alpha^{p-1} \mu_{(2:d+1)}^{\top} \end{pmatrix},
$$

$$
r_{\mathrm{time}}(g) = g_1^{2p-2} = \alpha^{2p-2},
$$

with all terms explained in Section 3.1. Note, that we included the $f_{1,0}$-term in the first column of $H^1_{\mathbf{k}}$. We also impose (29) to implement no-flux boundary conditions. As before $v_{\mathbb{K}} = (v_{\mathbf{k}})_{\mathbf{k} \in \mathbb{K}}$ is replaced

by $\widehat{u}_{\mathbb{K}} = (\widehat{u}_{\mathbf{k}})_{\mathbf{k} \in \mathbb{K}}$ in $H^{i,j}_{\mathbf{k}^j \pm \frac{1}{2}}$ and $f_{1,0}$ for the definition of $H^1(\widehat{u}_{\mathbb{K}})$. Equation (33) is written in matrix times vector from, where we understand $H^0(v_{\mathbb{K}})$, $f^1(v_{\mathbb{K}})$, and $P(v_{\mathbb{K}})$ as vectors in $\mathbb{R}^{\#(\mathbb{K})}$ and $H^1(v_{\mathbb{K}})$ as a matrix in $\mathbb{R}^{\#(\mathbb{K}),d+1}$, with $\#(\mathbb{K})$ being the number of elements in the index set $\mathbb{K}$.

4. Implementation of the Numerical Freezing Method II: Time Discretization

In this Section we introduce a new time-discretization of the DAE (33). First we motivate and explain our scheme and in then we analyze the local truncation error introduced by it. Note that for a full convergence analysis the PDE-approximation error has to be analyzed and one has to cope with the unbounded operators. We finish this section by a description of how the implicit equations can efficiently be solved.

4.1. An Implicit-Explicit Runge-Kutta Scheme.
Originating from the structure of the original problem (20a), see Remark 2.2, the ODE-part (33a) of (33) has very different components:
The $P(v_{\mathbb{K}})$-part is linear in $v_{\mathbb{K}}$, but as the discretization of a (negative) elliptic operator has spectrum which extends far into the left complex half plane. Therefore, the "sub-problem" $v'_{\mathbb{K}} = P(v_{\mathbb{K}})$ becomes very stiff for fine spatial grids and an efficient numerical scheme requires an implicit time discretization. On the other hand, the terms $H^0(v_{\mathbb{K}})$ and $H^1(v_{\mathbb{K}})\mu$ are highly nonlinear in the argument $v_{\mathbb{K}}$ due to the nonlinearity f and the reconstruction of a piecewise linear function from cell averages, see (24), (26) and Appendix A. But these terms, which originate from the spatial discretization of a hyperbolic problem, have a moderate CFL number, which scales linearly with the spatial stepsize, so that the "sub-problem" $v'_{\mathbb{K}} = -H^0(v_{\mathbb{K}}) - H^1(v_{\mathbb{K}})\mu$ is most efficiently implemented by an explicit time marching scheme.
To couple these contrary requirements, we introduce a $\frac{1}{2}$-explicit IMEX-Runge-Kutta time-discretization for coupled DAEs of the form (33). For $\frac{1}{2}$-explicit Runge-Kutta schemes for DAE problems, see [7].
To simplify the notation we write V for $v_{\mathbb{K}}$ and restrict the discussion mainly to (33a) and (33b), because (33c) and (33d) decouple. Hence, consider an ordinary DAE of the form

$$
\begin{aligned}
V' &= P(V) - H^1(V)\mu - H^0(V) + G(V), \\
0 &= H^1(V)^\top \Big(P(V) - H^1(V)\mu - H^0(V) + G(V) \Big)
\end{aligned}
\tag{34}
$$

in the case of the orthogonal phase condition (18) (resp. (31)) and

$$
\begin{aligned}
V' &= P(V) - H^1(V)\mu - H^0(V) + G(V), \\
0 &= \Psi^\top V - \Psi^\top \widehat{U}
\end{aligned}
\tag{35}
$$

in the case of the fixed phase condition (19) (resp. (32)).
From now on, consider general DAEs of the form (34) or (35), i.e. P, H^1, H^0, and G are given nonlinear functions of V, sufficiently smooth in their arguments.
Let two Butcher-tableaux be given,

$$
\text{Tableau 1:} \quad \begin{array}{c|c} c & A \\ \hline & b^\top \end{array} \qquad\qquad \text{Tableau 2:} \quad \begin{array}{c|c} c & \widehat{A} \\ \hline & \widehat{b}^\top \end{array}
$$

with $c = (c_0, \ldots, c_s)^\top$, $A = (a_{ij})_{i,j=0,\ldots,s}$, $\widehat{A} = (\widehat{a}_{ij})_{i,j=0,\ldots,s}$ and $b = (a_{s0}, \ldots, a_{ss})^\top$, $\widehat{b} = (\widehat{a}_{s0}, \ldots, \widehat{a}_{ss})^\top$.
We assume, that the Runge-Kutta method with Tableau 1 is explicit, and the Runge-Kutta method with Tableau 2 is diagonally implicit, i.e. $a_{ij} = 0$ for all $j \geq i$ and $\widehat{a}_{ij} = 0$ for all $j > i$.
Now assume that at some time instance τ_n a consistent approximation V^n and μ^n of V and μ is given. A step for (34) from τ_n to $\tau_{n+1} = \tau_n + h$ with stepsize h is then performed as follows:

$$
\text{Set} \quad V_0 = V^n
$$

and for $i = 1, \ldots, s$ the internal values V_i and μ_{i-1} of the scheme are given as solutions to

$$
(36) \quad \begin{cases} V_i = V_0 - h \sum_{\nu=0}^{i-1} a_{i\nu}\Big(H^1(V_\nu)\mu_\nu + H^0(V_\nu) - G(V_\nu)\Big) + h \sum_{\nu=0}^{i} \widehat{a}_{i\nu} P(V_\nu), \\ 0 = H^1(V_{i-1})^\top \Big(P(V_{i-1}) - H^1(V_{i-1})\mu_{i-1} - H^0(V_{i-1}) + G(V_{i-1})\Big), \end{cases} \quad i = 1, \ldots, s.
$$

As approximation of V at the new time instance τ_{n+1}

$$\text{set} \quad V^{n+1} := V_s.$$

A suitable approximation of μ^{n+1} at the new time instance is actually the internal value μ_0 of the next time instance, i.e. $\mu = \mu^{n+1}$ solves $0 = H^1(V^{n+1})^\top\big(P(V^{n+1}) - H^1(V^{n+1})\mu - H^0(V^{n+1}) + G(V^{n+1})\big)$. Similarly, a step for (35) is performed as follows:

$$\text{Set} \quad V_0 = V^n$$

and for $i = 1, \ldots, s$ let the internal values V_i and μ_{i-1} be given as solutions to

$$
(37) \quad \begin{cases} V_i = V_0 - h \sum_{\nu=0}^{i-1} a_{i\nu}\Big(H^1(V_\nu)\mu_\nu + H^0(V_\nu) - G(V_\nu)\Big) + h \sum_{\nu=0}^{i} \widehat{a}_{i\nu} P(V_\nu), \\ 0 = \Psi^\top V_i - \Psi^\top \widehat{U}, \end{cases} \quad i = 1, \ldots, s.
$$

In this case we set

$$V^{n+1} := V_s \text{ and } \mu^{n+1} := \mu_{s-1}$$

as approximations of V and μ at the new time instance $\tau_{n+1} = \tau_n + h$.

Remark 4.1. (i) A suitable time-discretization for the "parabolic sub-problem" $v'_{\mathbb{K}} = P(v_{\mathbb{K}})$ is the Crank-Nicolson method, for which there is no CFL-restriction and the resulting full discretization of $v' = \Delta v$ is of second order.

(ii) Concerning the semi-discrete "hyperbolic sub-problem" $v'_{\mathbb{K}} = -H^0(v_{\mathbb{K}}) - H^1(v_{\mathbb{K}})\mu$, it is shown in [10, Thm. 5.1] that an explicit Euler-Discretization with a suitable CFL-condition satisfies a stability property in form of a maximum principle (cf. non-oscillatory). It is possible to retain this property for higher order methods, if they can be written as convex combinations of explicit Euler steps. A simple second order method, for which this is possible is Heun's method, see [10, Cor. 5.1]. It was observed already in [17] that Heun's method is the optimal (concerning the CFL-restrictions) second order explicit Runge-Kutta type scheme.

For concreteness and motivated by Remark 4.1, we choose

$$
(38) \quad c = \begin{pmatrix} 0 \\ 1 \\ 1 \end{pmatrix}, \; A = \begin{pmatrix} 0 & 0 & 0 \\ 1 & 0 & 0 \\ \frac{1}{2} & \frac{1}{2} & 0 \end{pmatrix}, \; b^\top = \big(\tfrac{1}{2}, \tfrac{1}{2}, 0\big), \; \widehat{A} = \begin{pmatrix} 0 & 0 & 0 \\ \frac{1}{2} & \frac{1}{2} & 0 \\ \frac{1}{2} & 0 & \frac{1}{2} \end{pmatrix}, \; \widehat{b}^\top = \big(\tfrac{1}{2}, 0, \tfrac{1}{2}\big),
$$

i.e. we couple Heun's method with the Crank-Nicolson method.

As noted above, the ODEs (33c) and (33d) can be solved in a post-processing step, but if these values are also required, it is more convenient to do the calculation in parallel and use the same explicit scheme with Tableau 1 because the intermediate stages of V and μ are already calculated. Therefore, given the state g^n and t^n at τ_n, we perform a time step for (33c) and (33d) from τ_n to $\tau_{n+1} = \tau_n + h$ by

$$\text{let} \quad g_0 = g^n, \; t_0 = t^n,$$

compute for $i = 1, \ldots, s$

$$g_i = g_0 + h \sum_{\nu=0}^{i-1} a_{i\nu} r_{\text{alg}}(g_\nu, \mu_\nu), \quad t_i = t_0 + h \sum_{\nu=0}^{i-1} a_{i\nu} r_{\text{time}}(g_\nu)$$

and set

$$g^{n+1} := g_s, \quad t^{n+1} := t_s.$$

4.2. Order of the Time Discretization.

Now we consider the local truncation error of our IMEX-RK scheme for DAEs (36), resp. (37), with tableaux (38). Hence, consider an ordinary differential equation

$$(39) \qquad V' = P(V) + H(V, \mu), \quad g' = r_{\mathrm{alg}}(\mu, g), \quad t' = r_{\mathrm{time}}(g),$$

coupled to a system of algebraic equations of the form

$$(40a) \qquad 0 = \Psi(V, \mu),$$

or of the form

$$(40b) \qquad 0 = \Psi(V).$$

We assume that for consistent initial data $V(0) = V^0$, $g(0) = g^0$, $t(0) = t^0$, $\mu(0) = \mu^0$ a smooth solution $V \in \mathcal{C}^3([0,T]; \mathbb{R}^m)$, $\mu \in \mathcal{C}^3([0,T]; \mathbb{R}^p)$ of (39,40a) resp. (39,40b) exists. Furthermore we assume

Hypothesis 1. (i) *In the case of* (39) *with* (40a) *the matrix* $\partial_\mu \Psi\big(V(\tau), \mu(\tau)\big)$ *is invertible for any* $\tau \in [0, T)$.
(ii) *In the case of* (39) *with* (40b) *the matrix* $\partial_V \Psi\big(V(\tau)\big) \partial_\mu H\big(V(\tau), \mu(\tau)\big)$ *is invertible for any* $\tau \in [0, T)$.

It is easy to check that under Hypothesis 1 the system (39, 40a) is a DAE of (differentiation) index 1 and the system (39, 40b) is a DAE of (differentiation) index 2 (cf. [8, Ch. VII]).

Given consistent data V^n, g^n, t^n of the DAE (39, 40a) or (39, 40b) at some time-instance τ_n, a step of size h of the method with these data takes the following explicit form: Solve the system

$$(41a) \qquad V_0 = V^n, \quad g_0 = g^n, \quad t_0 = t^n,$$

$$(41b) \qquad \begin{bmatrix} V_1 = V_0 + \frac{h}{2}P(V_0) + \frac{h}{2}P(V_1) + hH(V_0, \mu_0), \\[4pt] 0 = \begin{cases} \Psi(V_0, \mu_0), & \text{case (40a), or} \\ \Psi(V_1), & \text{case (40b),} \end{cases} \\[8pt] g_1 = g_0 + hr_{\mathrm{alg}}(\mu_0, g_0), \\[4pt] t_1 = t_0 + hr_{\mathrm{time}}(g_0), \end{bmatrix}$$

$$(41c) \qquad \begin{bmatrix} V_2 = V_0 + \frac{h}{2}P(V_0) + \frac{h}{2}P(V_2) + \frac{h}{2}H(V_0, \mu_0) + \frac{h}{2}H(V_1, \mu_1), \\[4pt] 0 = \begin{cases} \Psi(V_1, \mu_1), & \text{case (40a), or} \\ \Psi(V_2), & \text{case (40b),} \end{cases} \\[8pt] g_2 = g_0 + \frac{h}{2}r_{\mathrm{alg}}(\mu_0, g_0) + \frac{h}{2}r_{\mathrm{alg}}(\mu_1, g_1), \\[4pt] t_2 = t_0 + \frac{h}{2}r_{\mathrm{time}}(g_0) + \frac{h}{2}r_{\mathrm{time}}(g_1). \end{bmatrix}$$

Finally, the values at the new time-instance $\tau^{n+1} = \tau^n + h$ are given by

$$(42) \quad V^{n+1} := V_2, \; g^{n+1} := g_2, \; t^{n+1} := t_2, \; \text{and} \, \mu^{n+1} \begin{cases} \text{by solving } \Psi(V^{n+1}, \mu^{n+1}) = 0, & \text{case (40a),} \\ \mu_1, & \text{case (40b).} \end{cases}$$

Since the g- and t-equation decouple from the system, we first consider the V and μ variables separately. To analyze the local error, we assume that $(V_\star, \mu_\star)$ is a given consistent value at $\tau = 0$, so that the DAE satisfies all assumptions from above with (V^0, μ^0) replaced by $(V_\star, \mu_\star)$. For brevity, a subindex $\star$ denotes the evaluation of a function at $\tau = 0$, e.g. $(V_\star, \mu_\star) = (V(0), \mu(0))$, $\partial_V P_\star = \frac{\partial}{\partial V}P(V(0))$.

Taylor expansion of the exact solution. First we consider the differential variables V and obtain from the ODE (39) and anticipating $\mu(0) = \mu_\star$ (see (44a), resp. (45b), below)

$$(43\text{a}) \qquad\qquad\qquad V(0) = V_\star,$$

$$(43\text{b}) \qquad\qquad\qquad V'(0) = P_\star + H_\star =: V'_\star,$$

$$(43\text{c}) \qquad\qquad\qquad V''(0) = \partial_V P_\star V'_\star + \partial_V H_\star V'_\star + \partial_\mu H_\star \mu'(0) =: V''_\star.$$

Similarly, we can use the differential equation (39) together with the algebraic constraint (40a) to obtain in the index-1 case for the algebraic variable

$$(44\text{a}) \qquad\qquad 0 = \Psi(V_\star, \mu_\star), \quad \text{(locally unique solvable for } \mu_\star \text{ by Hypothesis 1 (i))},$$

$$(44\text{b}) \qquad \mu'(0) = -\left(\partial_\mu \Psi_\star\right)^{-1} \partial_V \Psi_\star \left(P_\star + H_\star\right) =: \mu'_\star,$$

$$(44\text{c}) \qquad \mu''(0) = -\left(\partial_\mu \Psi_\star\right)^{-1} \left\{ \partial_V^2 \Psi_\star V'^2_\star + \partial_V \Psi_\star V''_\star + 2\partial_V \partial_\mu \Psi_\star V'_\star \mu'_\star + \partial_\mu^2 \Psi_\star \mu'^2_\star \right\} =: \mu''_\star.$$

For the index-2 case (i.e. (40b)) the first coefficients of the Taylor expansion of the algebraic variables μ are obtained by differentiating the algebraic condition (40b) and using the ODE (39) to find

$$(45\text{a}) \qquad\qquad 0 = \Psi(V_\star),$$

$$(45\text{b}) \qquad\qquad 0 = \partial_V \Psi_\star (P_\star + H_\star), \quad \text{(locally unique solvable for } \mu_\star \text{ by Hypothesis 1 (ii))},$$

$$(45\text{c}) \qquad \mu'(0) = -\left(\partial_V \Psi_\star \partial_\mu H_\star\right)^{-1} \left\{ \partial_V^2 \Psi_\star V'^2_\star + \partial_V \Psi_\star \partial_V P_\star V'_\star + \partial_V \Psi_\star \partial_V H_\star V'_\star \right\} =: \mu'_\star.$$

Taylor expansion of the numerical solution. We assume that the numerical solution and all intermediate stages depend smoothly on the step-size h. To emphasize this dependence, we explicitly include the dependence on h in the notation.

First consider the differential variable V, anticipating that the algebraic variables $\mu_0(h)$ and $\mu_1(h)$ are known and satisfy $\mu_0(0) = \mu_1(0) = \mu_\star$, which will be justified in (50) and (51), resp. (55) and (57). By (41) the numerical values $V_1(h)$ and $V_2(h)$ satisfy

$$(46) \qquad \begin{aligned} V_1(h) &= V_0 + \tfrac{h}{2}P(V_0) + \tfrac{h}{2}P(V_1(h)) + hH(V_0, \mu_0(h)) \\ &= V_\star + \tfrac{h}{2}P_\star + \tfrac{h}{2}P(V_1(h)) + hH(V_\star, \mu_0(h)), \\ V_2(h) &= V_0 + \tfrac{h}{2}P(V_0) + \tfrac{h}{2}P(V_2(h)) + \tfrac{h}{2}H(V_0, \mu_0(h)) + \tfrac{h}{2}H(V_1(h), \mu_1(h)) \\ &= V_\star + \tfrac{h}{2}P_\star + \tfrac{h}{2}P(V_2(h)) + \tfrac{h}{2}H(V_\star, \mu_0(h)) + \tfrac{h}{2}H(V_1(h), \mu_1(h)). \end{aligned}$$

For the differential variables we then obtain for the first intermediate stage:

$$(47\text{a}) \qquad V_1(0) = V_\star,$$

$$(47\text{b}) \qquad V_1'(h) = \tfrac{1}{2}P_\star + \tfrac{1}{2}P(V_1(h)) + \tfrac{h}{2}\partial_V P(V_1(h))V_1'(h) + H(V_\star, \mu_0(h)) + h\partial_\mu H(V_\star, \mu_0(h))\mu_0'(h),$$

$$(47\text{c}) \qquad V_1'(0) = P_\star + H_\star = V'_\star,$$

$$(47\text{d}) \qquad V_1''(0) = \partial_V P_\star (P_\star + H_\star) + 2\partial_\mu H_\star \mu_0'(0).$$

Similarly, for the final (second) stage we obtain

$$(48\text{a}) \qquad V_2(0) = V_\star,$$

$$(48\text{b}) \qquad \begin{aligned} V_2'(h) = {}&\tfrac{1}{2}P_\star + \tfrac{1}{2}P(V_2(h)) + \tfrac{h}{2}\partial_V P(V_2(h))V_2'(h) + \tfrac{1}{2}H(V_\star, \mu_0(h)) + \tfrac{h}{2}\partial_\mu H(V_\star, \mu_0(h))\mu_0'(h) \\ &+ \tfrac{1}{2}H(V_1(h), \mu_1(h)) + \tfrac{h}{2}\partial_V H(V_1(h), \mu_1(h))V_1'(h) + \tfrac{h}{2}\partial_\mu H(V_1(h), \mu_1(h))\mu_1'(h), \end{aligned}$$

$$(48\text{c}) \qquad V_2'(0) = P_\star + H_\star = V'_\star,$$

$$(48\text{d}) \qquad V_2''(0) = \partial_V P_\star (P_\star + H_\star) + \partial_V H_\star (P_\star + H_\star) + \partial_\mu H_\star (\mu_0'(0) + \mu_1'(0)).$$

14

Now we consider the Taylor expansion of the numerical solution of the algebraic variables. We begin with the *index*-1 *case*, i.e. (46) is closed by imposing the algebraic constraints

$$(49) \qquad 0 = \Psi(V_0(h), \mu_0(h)), \quad 0 = \Psi(V_1(h), \mu_1(h)).$$

Since $V_0(h) = V_\star$ for all $h \geq 0$, (49) implies because of Hypothesis 1 (i)

$$(50) \qquad \mu_0(h) = \mu_\star \text{ and } \mu_0'(h) = 0 \ \forall h \geq 0.$$

This justifies (47) and shows $V_1''(0) = \partial_V P_\star(P_\star + H_\star)$. Then we can calculate the Taylor expansion of $\mu_1(h)$ around 0 from (49) to find

$$(51) \quad \begin{aligned} 0 &= \Psi(V_1(h), \mu_1(h)) & \text{which implies } \mu_1(0) = \mu_\star \text{ since } V_1(0) = V_\star, \\ 0 &= \partial_V \Psi_1 V_1' + \partial_\mu \Psi_1 \mu_1' & \text{which implies } \mu_1'(0) = -\big(\partial_\mu \Psi_\star\big)^{-1} \partial_V \Psi_\star(P_\star + H_\star) = \mu_\star' \text{ from (44b).} \end{aligned}$$

Thus, inserting the findings for $\mu_0'(0)$ and $\mu_1'(0)$ into the Taylor expansion of V_2, (48), shows $V_2(0) = V_\star$, $V_2'(0) = V_\star'$, and $V_2''(0) = V_\star''$, which proves for the differential variable V_2 second order consistency,

$$(52) \qquad V_2(h) = V(h) + \mathcal{O}(h^3) \quad \text{as } h \searrow 0.$$

Setting $\mu_2(h)$ as solution of $\Psi(V_2(h), \mu_2(h)) = 0$ implies also second order for the algebraic variable

$$(53) \qquad \mu_2(h) = \mu(h) + \mathcal{O}(h^3) \quad \text{as } h \searrow 0.$$

In the *index*-2 *case* (46) is closed by appending the algebraic constraints

$$(54) \qquad 0 = \Psi\big(V_1(h)\big), \quad 0 = \Psi\big(V_2(h)\big).$$

Differentiating the first of these two equations yields $0 = \partial_V \Psi(V_1(h)) V_1'(h)$ and at $h = 0$

$$(55) \qquad 0 = \partial_V \Psi_\star\big(P_\star + H(V_\star, \mu_0(0))\big),$$

which by Hypothesis 1 (ii) has the locally unique solution $\mu_0(0) = \mu_\star$. Considering the second derivative at $h = 0$ leads to

$$0 = \partial_V^2 \Psi_\star(P_\star + H_\star)^2 + \partial_V \Psi_\star\big(\partial_V P_\star(P_\star + H_\star) + 2\partial_\mu H_\star \mu_0'(0)\big),$$

so that

$$(56) \qquad \mu_0'(0) = -\big(\partial_V \Psi_\star \partial_\mu H_\star\big)^{-1}\Big\{\tfrac{1}{2}\partial_V^2 \Psi_\star(P_\star + H_\star)^2 + \tfrac{1}{2}\partial_V \Psi_\star\big(\partial_V P_\star(P_\star + H_\star)\big)\Big\}.$$

Similarly, differentiating the second equation in (54) once and evaluating at $h = 0$ yields

$$0 = \partial_V \Psi_\star\big(P_\star + \tfrac{1}{2}H_\star + \tfrac{1}{2}H(V_\star, \mu_1(0))\big),$$

which has the locally unique solution

$$(57) \qquad \mu_1(0) = \mu_\star.$$

Considering the second derivative at $h = 0$, inserting (48d) and comparing with (45c) shows

$$(58) \qquad \mu_0'(0) + \mu_1'(0) = \mu_\star'.$$

Therefore, we obtain again (52) for V_2. But for the algebraic variables we only find the estimate

$$(59) \qquad \mu_1(h) + \mathcal{O}(h) = \mu_2(h) + \mathcal{O}(h) = \mu(h) \quad \text{as } h \searrow 0,$$

which is a severe order reduction.

Nevertheless, when the group variables g and the transformed time t are calculated in parallel with V and μ, these variables are again second order accurate, i.e.

$$(60) \qquad g_2(h) = g(h) + \mathcal{O}(h^3), \quad t_2(h) = t(h) + \mathcal{O}(h^3) \quad \text{as } h \searrow 0.$$

This can be seen, by either including the equations $g' = r_{\text{alg}}(\mu, g)$ and $t' = r_{\text{time}}(g)$ into the V-equation, or by performing a similar analysis as above.

Summarizing the above analysis we obtain.

Theorem 4.2. *Assume that the DAE consisting of the ODE system* (39) *and either* (40a) *or* (40b) *with consistent initial data* $(V_\star, \mu_\star, g_\star, t_\star)$ *at* $\tau = \tau_n$ *has a smooth solution in some non-empty interval* $[\tau_n, T)$ *and satisfies Hypothesis* 1. *Then the method* (41), (42) *is consistent of second order at the differential variables, i.e.* (52) *and* (60) *hold. Moreover, in the case of* (40a) *also the algebraic variables* μ *are second order consistently approximated, i.e.* (53) *holds.*

Remark 4.3. We observe here the well-known difficulty with higher index problems, that one faces a loss in the order of the approximation of the algebraic variables. But note, that one is often mainly interested in the behavior of the original solution, so that the approximation of μ is not important but the approximations of V, g, and t are crucial.

Moreover, when the main focus is on the asymptotic behavior and the final rest state, one is interested in the limit $\lim_{\tau \to \infty} \mu(\tau)$ but not on its actual evolution. The approximation of this is actually not dependent on the time-discretization but only on the spatial discretization, because we are using a Runge-Kutta-type method. In fact, in this case it might even be better to use a scheme which has a less restrictive CFL condition but maybe has a lower order in the time approximation. See [16] for such ideas in the case of hyperbolic conservation laws.

4.3. Efficiently solving the Runge-Kutta Equations.
We remark that in Burgers' case and similar cases with a linear operator P, the actual equations (36) and (37) from the IMEX-time-discretization can be solved very efficiently. To see this, we write (36) in block-matrix form

$$
(61) \qquad \begin{pmatrix} I - h\,\widehat{a}_{i,i}P & h\,a_{i,i-1}\,H^1(V_{i-1}) \\ 0 & H^1(V_{i-1})^\top H^1(V_{i-1}) \end{pmatrix} \begin{pmatrix} V_i \\ \mu_{i-1} \end{pmatrix} = \begin{pmatrix} R_i^1 \\ R_i^2 \end{pmatrix}, \quad i = 1, \ldots, s,
$$

where $R_i^1 = R_i^1(V_0, \ldots, V_{i-1}, \mu_0, \ldots, \mu_{i-2})$ and $R_i^2 = R_i^2(V_{i-1})$ are given by

$$
R_i^1 = V_0 - h\left(\sum_{\nu=0}^{i-2} a_{i\nu} H^1(V_\nu)\mu_\nu + \sum_{\nu=0}^{i-1} a_{i\nu}\big(H^0(V_\nu) - G(V_\nu)\big) - \sum_{\nu=0}^{i-1} \widehat{a}_{i\nu} P(V_\nu) \right),
$$
$$
R_i^2 = H^1(V_{i-1})^\top \big(P(V_{i-1}) - H^0(V_{i-1}) + G(V_{i-1}) \big).
$$

A solution to (61) can be calculated by solving for each $i = 1, \ldots, s$ one small linear system with the $(d+1) \times (d+1)$-matrix $H^1(V^{(i-1)})^\top H^1(V^{(i-1)})$ and one large linear system with the matrix $I - h\,\widehat{a}_{i,i}P$. Similarly, (37) can be written in the block-matrix form

$$
(62) \qquad \begin{pmatrix} I - h\,\widehat{a}_{i,i}\,P & h\,a_{i,i-1}\,H^1(V_{i-1}) \\ \Psi^\top & 0 \end{pmatrix} \begin{pmatrix} V_i \\ \mu_{i-1} \end{pmatrix} = \begin{pmatrix} R_i^1 \\ R^2 \end{pmatrix}, \quad i = 1, \ldots, s,
$$

where R_i^1 is given as above and $R^2 = \Psi^\top \widehat{U}$ does not depend on the stage i. It is possible to obtain a solution to (62) by solving $d+2$ large linear systems with $I - h\,\widehat{a}_{i,i}P$ and one small linear $(d+1) \times (d+1)$ system:

$$
\begin{aligned}
A_\star &= \big(I - h\,\widehat{a}_{i,i}P\big)^{-1} h a_{i,i-1} H^1(V_{i-1}), && ((d+1)\times \text{ large}) \\
V_\star &= \big(I - h\,\widehat{a}_{i,i}P\big)^{-1} R_i^1, && (1\times \text{ large}) \\
\mu_{i-1} &= \big(\Psi^\top A_\star\big)^{-1}\big(\Psi^\top V_\star - R^2\big), && (1\times \text{ small}) \\
V_i &= V_\star - A_\star \mu_{i-1}.
\end{aligned}
$$

Therefore, if h does not vary during computation, factorizations of $I - h\,\widehat{a}_{i,i}P$, $i = 1, \ldots, s$ can be calculated in a preprocessing step and then the subsequent time steps are rather cheap. Note that for our specific scheme with Butcher tableaux (38) holds $s = 2$ and $\widehat{a}_{1,1} = \widehat{a}_{2,2} = \frac{1}{2}$, so that only one matrix factorization is needed, namely of $I - h\frac{1}{2}P$.

5. Numerical experiments

In the current paper, we are primarily interested in the actual discretization of the freezing PDAE (20) and the error introduced by the discretization. We present results of several numerical experiments which support second order convergence of the method for the full discretization of the PDAE for our scheme.

For further numerical findings we refer to [14], where we use the same scheme and see that our method enables us to do long time simulations for Burgers' equation on fixed (bounded) computational domains also for different parameter values of $p > 1$ in (6). We also note that our method is also able to capture the meta-stable solution behavior present in (6) for the case $0 < \nu << |a|$ and again refer to [14]. Note that in that paper we completely ignored the errors introduced by the discretization.

In the following, we restrict to the special choice $p = \frac{d+1}{d}$ in (6). For convenience we explicitly state the systems for freezing similarity solutions of the "*conservative*" Burgers' equation (i.e. $p = \frac{d+1}{d}$) in one and two spatial dimensions. These are the systems we numerically solve with the scheme proposed in Sections 3–4. In the **1d case** we solve the PDAE system

$$
(63) \quad
\begin{cases}
v_\tau = \nu v_{\xi\xi} - \frac{1}{2}\left(v^2\right)_\xi + \mu_1(\xi v)_\xi + \mu_2 v_\xi, \quad v(0) = u_0, \\
0 = \Psi(v, \mu) \in \mathbb{R}^2, \\
\alpha_\tau = \alpha\mu_1,\ b_\tau = \alpha\mu_2,\ t_\tau = \alpha^2, \qquad \alpha(0) = 1,\ b(0) = 0,\ t(0) = 0.
\end{cases}
$$

And the functional Ψ is either given by

$$
\Psi(v, \mu) = \begin{pmatrix} \int_{\mathbb{R}} (\xi v)_\xi \cdot \left(\nu v_{\xi\xi} - \frac{1}{2}(v^2)_\xi + \mu_1(\xi v)_\xi + \mu_2 v_\xi\right) d\xi \\ \int_{\mathbb{R}} v_\xi \cdot \left(\nu v_{\xi\xi} - \frac{1}{2}(v^2)_\xi + \mu_1(\xi v)_\xi + \mu_2 v_\xi\right) d\xi \end{pmatrix} \quad \text{(orthogonal phase condition)}
$$

or by

$$
\Psi(v) = \begin{pmatrix} \int_{\mathbb{R}} (\xi v)_\xi \cdot \left(\widehat{u} - v\right) d\xi \\ \int_{\mathbb{R}} v_\xi \cdot \left(\widehat{u} - v\right) d\xi \end{pmatrix} \quad \text{(fixed phase condition)}.
$$

Similarly, in the **2d case** we numerically solve

$$
(64) \quad
\begin{cases}
v_\tau = \underbrace{\nu\, \Delta v - \frac{2}{3}\left(\partial_{\xi_1} + \partial_{\xi_2}\right)|v|^{\frac{3}{2}} + \frac{1}{2}\mu_1\big((\xi_1 v)_{\xi_1} + (\xi_2 v)_{\xi_2}\big) + \mu_2 v_{\xi_1} + \mu_3 v_{\xi_2}}_{=:\text{RHS}(v,\mu)}, \quad v(0) = u_0 \\
0 = \Psi(v, \mu) \in \mathbb{R}^3, \\
\alpha_\tau = \alpha\mu_1,\ b_{1,\tau} = \alpha^{\frac{1}{2}}\mu_2,\ b_{2,\tau} = \alpha^{\frac{1}{2}}\mu_3,\ t_\tau = \alpha, \quad \alpha(0) = 1,\ b_1(0) = 0,\ b_2(0) = 0,\ t(0) = 0.
\end{cases}
$$

The functional Ψ is either given by

$$
\Psi(v, \mu) = \begin{pmatrix} \int_{\mathbb{R}^2} \big((\xi_1 v)_{\xi_1} + (\xi_2 v)_{\xi_2}\big) \cdot \text{RHS}(v, \mu)\, d\xi \\ \int_{\mathbb{R}^2} v_{\xi_1} \cdot \text{RHS}(v, \mu)\, d\xi \\ \int_{\mathbb{R}^2} v_{\xi_2} \cdot \text{RHS}(v, \mu)\, d\xi \end{pmatrix} \quad \text{(orthogonal phase condition)}
$$

or by

$$
\Psi(v) = \begin{pmatrix} \int_{\mathbb{R}^2} \big((\xi_1 v)_{\xi_1} + (\xi_2 v)_{\xi_2}\big) \cdot \left(\widehat{u} - v\right) d\xi \\ \int_{\mathbb{R}^2} v_{\xi_1} \cdot \left(\widehat{u} - v\right) d\xi \\ \int_{\mathbb{R}^2} v_{\xi_2} \cdot \left(\widehat{u} - v\right) d\xi \end{pmatrix} \quad \text{(fixed phase condition)}.
$$

In the following we write $\Delta\tau$ for the time step-size h and $\Delta\xi$, resp. $\Delta\xi_1$ and $\Delta\xi_2$, for the spatial step-sizes.
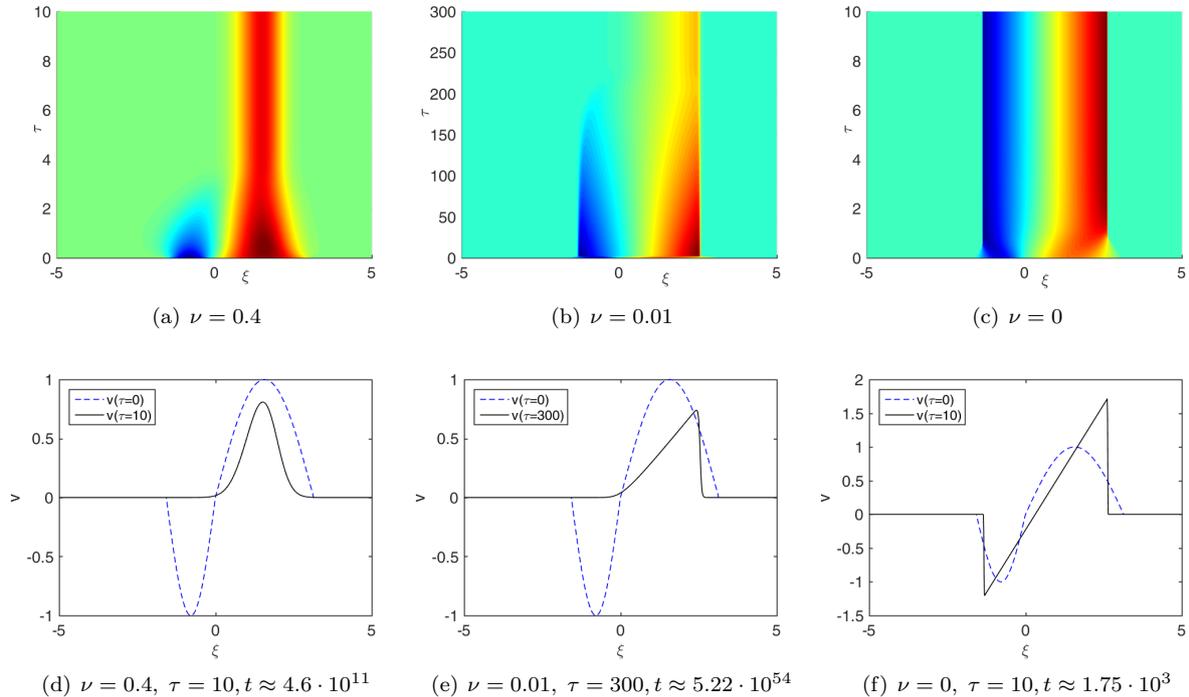
FIGURE 1. Time evolution (a)–(c) and final states after the solution stabilized (d)–(f) for the freezing method for 1d-Burgers' equation with different sizes of viscosity. The initial value is given by the dashed line, the final state by the solid line. All plots are in the scaled and translated coordinates of the freezing method.

5.1. **1d-Experiments.** We choose a fixed spatial domain Ω, as explained in Section 3.2. Due to the nonlinearity, and because the algebraic variables μ depend implicitly on the solution, we choose a very rough upper estimate for the value of $\mathbf{a}$ in (24) for simplicity. We take (cf. (30))

$$(65) \qquad \mathbf{a} \le \sup_{\xi \in \Omega} |v(\xi)| + |\mu_1| \max\{|\xi| : \xi \in \Omega\} + |\mu_2|,$$

where μ_1, μ_2 are the current approximations obtained in the last time step, so that the number $\mathbf{a}$ is updated after each time step.

As time step-size we choose $\Delta\tau$ which satisfies

$$(66) \qquad \Delta\tau \le \frac{\Delta\xi}{\mathbf{a}} \cdot \lambda_{\mathrm{CFL}},$$

so the time step-size may increase or decrease during the calculation, depending on the evolution of $\mathbf{a}$ from (65). Experimentally, we found that $\lambda_{\mathrm{CFL}} = \frac{1}{3}$ is a suitable choice for all spatial step-sizes $\Delta\xi$ and all viscosities $\nu \ge 0$. In our code we actually do not update $\Delta\tau$ after each step, but only if (66) is violated or $\Delta\tau$ might be enlarged significantly according to (66).

In Fig. 1(a)–(c) we show the time evolution of the solution to the freezing PDAE (63) for $\nu = 0.4$, $\nu = 0.01$ and $\nu = 0$. The initial function is $u_0(x) = \sin(2x)1_{[-\frac{\pi}{2},0]} + \sin(x)1_{[0,\pi]}$, where 1_A is the indicator function. One observes that the solution converges to a stationary profile as time increases. We stopped the calculation when the solution did not change anymore. The initial value together with the final state of these simulations is shown in Fig. 1(d)–(f). Note that in all plots the solution is given

in the co-moving coordinates of (63) and the solution in the original coordinates is obtained by the transformation $u(x,t) = \frac{1}{\alpha(\tau)} v(\frac{x-b(\tau)}{\alpha(\tau)}, \tau)$. At the final time the algebraic variables α and μ have the values $\alpha(10) \approx 1.2 \cdot 10^6$ and $b(10) \approx -1.6 \cdot 10^6$ in Fig. 1(d), $\alpha(300) \approx 1.3 \cdot 10^{27}$ and $b(300) \approx -1.8 \cdot 10^{26}$ in Fig. 1(e), $\alpha(10) \approx 36$ and $b(10) \approx -11$ for Fig. 1(f).

Order of the method. Now we numerically check the order of our method. For this we calculate the solution for different step-sizes $\Delta\xi$ until time $\tau = 1$ and compare the final state with a reference solution, obtained by using a much smaller step-size $\Delta\xi = 0.0005$. We calculate on the fixed spatial domain $[R^-, R^+]$ with no-flux boundary conditions as described in Section 3. We calculate the error

(a) $\nu = 1$, orthogonal phase

(b) $\nu = 0.01$, orthogonal phase

(c) $\nu = 1$, fixed phase
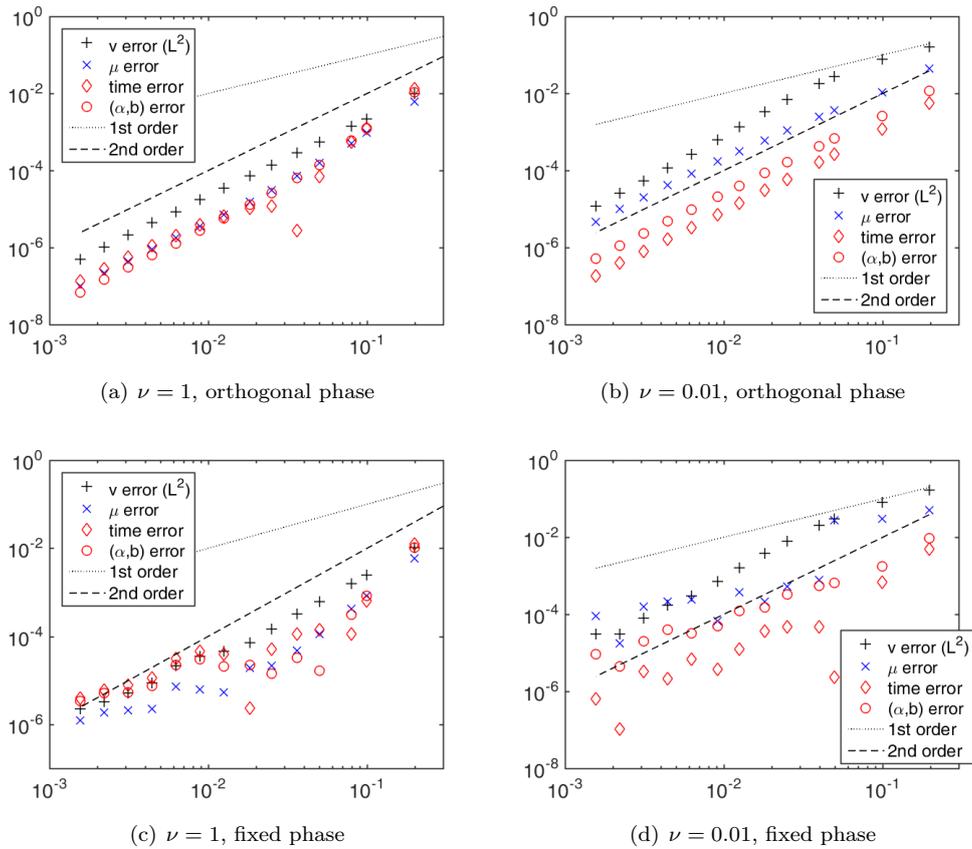
(d) $\nu = 0.01$, fixed phase

FIGURE 2. Convergence plots for freezing 1d-Burgers equation. With large viscosity left column) and very small viscosity (right column), and orthogonal phase condition (top row) and fixed phase condition (bottom row).

of all solution components separately. Namely we calculate the L^2-error of the differential variable ("v error") $\int_{R^-}^{R^+} |v_{\Delta\xi}(\xi,1) - v_{\text{ref}}(\xi,1)|^2 \, d\xi$, the error of the algebraic variables ("μ error") $|\mu_{\Delta\xi}(1) - \mu_{\text{ref}}(1)|_\infty$, the error of the reconstructed time ("time error") $|t_{\Delta\xi}(1) - t_{\text{ref}}(1)|$, and the error of the reconstructed transformation ("α, b error") $\max(|\alpha_{\Delta\xi}(1) - \alpha_{\text{ref}}(1)|, |b_{\Delta\xi}(1) - b_{\text{ref}}(1)|)$. Here a sub-index $\Delta\xi$ denotes the result of the numerical approximation with step-size $\Delta\xi$ and a sub-index ref refers to the reference solution. The results are shown in Fig. 2, where we consider large and small viscosities ($\nu = 1$ and $\nu = 0.01$) and in both cases orthogonal and fixed phase conditions. The results for other values of

viscosity ν look very similar and are not shown. In all experiments $\Delta\xi$ is prescribed, and $\Delta\tau$ is related to $\Delta\xi$, so that (66) holds, as described above. Moreover, we choose $R^+ = -R^- = 10$ for $\nu = 1$ and $R^+ = -R^- = 5$ for $\nu = 0.01$ so we may neglect the influece of the boundary conditions.

On the horizontal axis in Fig. 2 we plot the $\Delta\xi$-value and the vertical axis is the error of the respective solution components. In all experiments one observes second order convergence for the orthogonal phase condition, as was proved (for ODEs) in Theorem 4.2. One also observes second order convergence for the differential variables in case of the fixed phase condition, which was also shown in Theorem 4.2.

Violation of CFL condition. Our final experiment for the 1d Burgers' equation concerns violation of (66). In Fig. 3(a) we consider the inviscid equation and choose $\lambda_{\mathrm{CFL}} = 1.2$ in (66) (instead of $\lambda_{\mathrm{CFL}} = \frac{1}{3}$).

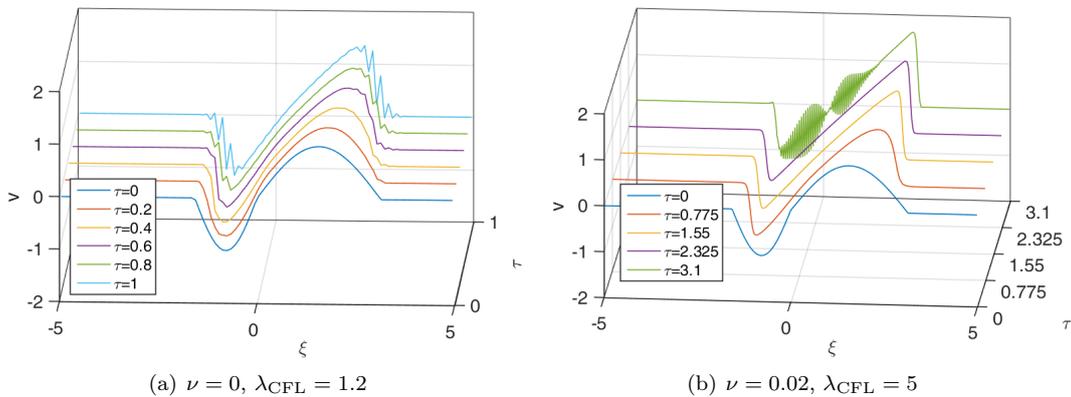(a) $\nu = 0$, $\lambda_{\mathrm{CFL}} = 1.2$ (b) $\nu = 0.02$, $\lambda_{\mathrm{CFL}} = 5$

FIGURE 3. Appearance of oscillations, when the ratio $\frac{\Delta\tau}{\Delta\xi}$ is too large.

The spatial stepsize is $\Delta\xi = 0.1$. One nicely observes how oscillations develop. Actually, the calculation breaks down soon after the plotted solution at $\tau = 1$. For this choice of λ_{CFL} we observed the same behavior also for all other step-sizes $\Delta\xi$ we have tried and we do not present these experiments here.

In Fig. 3(b) we show the result for $\nu = 0.02$. In this case we have chosen $\lambda_{\mathrm{CFL}} = 5$ in (66) and the spatial step-size was $\Delta\xi = 10/350$. Further experiments with different step-sizes $\Delta\xi$ seem to suggest that the numerical discretization of the parabolic part is strongly smoothing and there is no linear barrier of $(\Delta\tau)/(\Delta\xi)$ which prevents oscillations but rather the ratio may increase as $\Delta\xi$ decreases. Nevertheless, we expect that in the coupled hyperbolic-parabolic case the linear relation dominates.

5.2. **2d-Experiments.** We also apply our method to the following two-dimensional Burgers' equations

$$(67) \qquad \partial_t u = \nu \Delta u - \tfrac{2}{3}(\partial_x + \partial_y)\big(|u|^{\frac{3}{2}}\big).$$

That is, we numerically solve (64) with the scheme introduced in Sections 3–4. First we choose a fixed rectangular spatial domain Ω, as explained in Section 3.2. As in the one-dimensional case, we bound the maximal local wave speed by the rough upper estimate

$$(68) \qquad \mathbf{a} = \sup_{\xi \in \Omega} \sqrt{|v(\xi)|} + \max\big(|\mu_1| \max_{\xi \in \Omega} |\xi_1| + |\mu_2|, |\mu_1| \max_{\xi \in \Omega} |\xi_2| + |\mu_3|\big),$$

and choose in each time step a step-size $\Delta\tau$ so that

$$(69) \qquad \Delta\tau \leq \frac{\min(\Delta\xi_1, \Delta\xi_2)}{\mathbf{a}} \cdot \lambda_{\mathrm{CFL}}.$$

We found that $\lambda_{\mathrm{CFL}} = 0.2$ is a suitable choice. Note that in [10] there are bounds for λ_{CFL} given, which guarantee a maximum principle.

(a) Initial data   (b) Final state at $\tau = 6$ (c) Relative error at $\tau = 6$
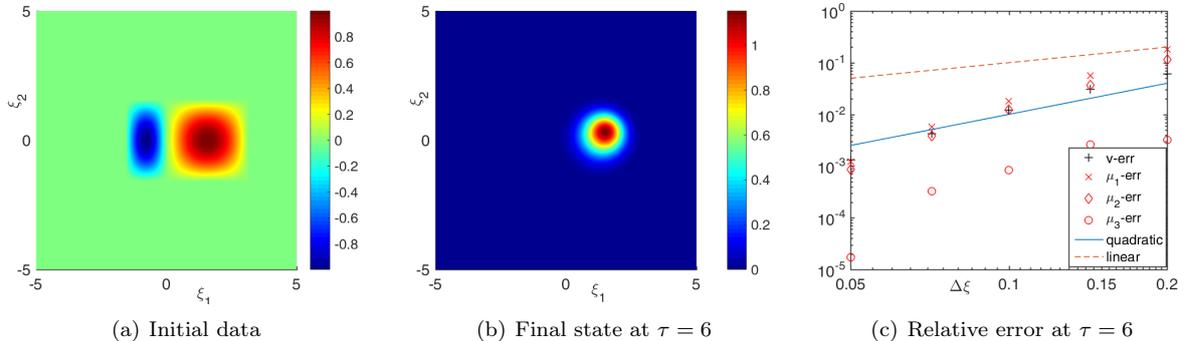
FIGURE 4. The final state of the reference solution $v_{\mathrm{ref}}(6)$ is shown in (b), it is obtained by the freezing method (64) with $\nu = 0.4$ and initial function shown in (a). In (c) we show the relative errors of solutions obtained on coarser grids compared to the solution on the fine grid.

Plots, showing the time evolution of the solution to the freezing method, calculated with our scheme can be found in [14] and we do not repeat them here, as we focus on the discretization and the error introduced by the discretization in the present article. In all our experiments we solve the Cauchy problem for (6) with initial data u_0, given by

$$u_0(x, y) = \begin{cases} \cos(y) \cdot \sin(2x), & -\frac{\pi}{2} < y < \frac{\pi}{2}, -\frac{\pi}{2} < x < 0, \\ \cos(y) \cdot \sin(x), & -\frac{\pi}{2} < y < \frac{\pi}{2}, 0 < x < \pi, \\ 0, & \text{otherwise,} \end{cases}$$

depicted in Fig. 4(a), by the freezing method (64). We choose the fixed domain $\Omega = [-5, 5]^2$ with no-flux boundary conditions.

In our first experiment we choose the viscosity $\nu = 0.4$ and solve the freezing system until $\tau = 6$, which is a time when the solution has settled. The final state of this calculation obtained for the fine grid with $\Delta\xi = \Delta\xi_1 = \Delta\xi_2 = \frac{1}{28}$ is shown in Fig. 4(b). We choose this solution as reference solution. In Fig. 4(c) we plot the difference of the solution components for different step-sizes. More precisely we plot the relative L^2-difference $\frac{1}{\|v_{\mathrm{ref}}\|}\|v_{\Delta\xi} - v_{\mathrm{ref}}\|$ ("v-err"), and the relative differences of the algebraic variables $\frac{1}{|\mu_{j,\mathrm{ref}}|}|\mu_{j,\Delta\xi} - \mu_{j,\mathrm{ref}}|$ ("μ_j error") at the final time $\tau = 6$. The numerical findings suggest that the scheme is in fact second order convergent (in $\Delta\xi$). We repeat the experiment with the very small viscosity $\nu = 0.05$. The solution to the 2d-Burgers' equation (67) with this viscosity and the same initial data as before shows a meta-stable behavior similar to the one-dimensional case. Therefore we have to calculate for a very long time and we show the final state of the calculation at time $\tau = 300$ for $\Delta\xi_1 = \Delta\xi_2 = 0.05$ in Fig. 5(a) and plot in Fig. 5(b),5(c) the deviation of solutions obtained for coarser grids with $\Delta\xi_1 = \Delta\xi_2 = 0.2$ and $\Delta\xi_1 = \Delta\xi_2 = 0.1$ from the reference solution.

In Figs. 6, 7 we again consider the solution to the freezing method for (67) with $\nu = 0.05$. We choose the solution with stepsize $\Delta\xi_1 = \Delta\xi_2 = 0.05$ as reference solution and plot for different step-sizes $\Delta\xi_1 = \Delta\xi_2 = dx$, how the error of the solution components depends on time. For all solution components the result is similar: One observes that the error initially rapidly increases, as it is expected since the error cumulates over time. But after a short time ($\tau \approx 6$) it settles and even slowly decreases lateron ($\tau \approx 100$) until it finally reaches a stationary value ($\tau \approx 150$).
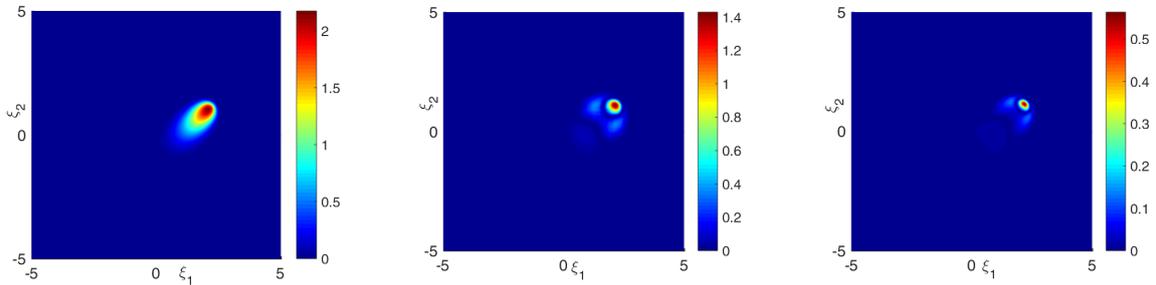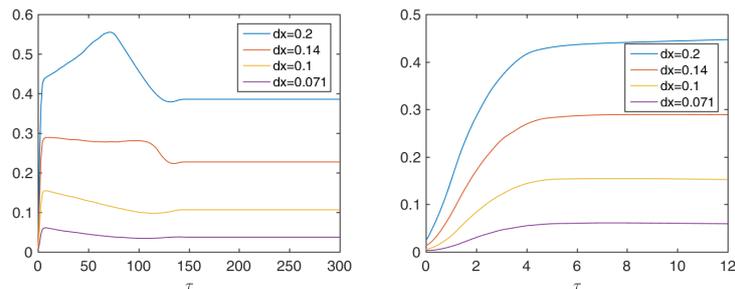
(a) Reference solution v_{ref} at $\tau = 300$ for cell size 0.05×0.05.

(b) Difference $v_{\mathrm{ref}} - v$.

(c) Difference $v_{\mathrm{ref}} - v$.

FIGURE 5. Comparison of the solutions obtained with the freezing method at $\tau = 300$ for $\nu = 0.05$ and different cell sizes, 0.2×0.2 vs. 0.05×0.05 in (b), and 0.1×0.1 vs. 0.05×0.05 in (c).

(a) Relative L^2-error depending on time.

(b) Zoom into initial behavior.

FIGURE 6. The relative L^2-error $\frac{1}{\|v_{\mathrm{ref}}(\tau)\|} \|v_{\mathrm{ref}}(\tau) - v(\tau)\|$ for different step-sizes $\Delta \xi_1 = \Delta \xi_2 = dx$ drawn as a function of time.

Violation of CFL condition. We also observed that oscillations appear, when we violate (69). We found that oscillations for example appear for the same problem with $\nu = 0.02$ and $\lambda_{\mathrm{CFL}} = 0.8$. But we do not present the results here.

REFERENCES

[1] U. M. Ascher, S. J. Ruuth, and R. J. Spiteri. Implicit-explicit Runge-Kutta methods for time-dependent partial differential equations. *Appl. Numer. Math.*, 25(2-3):151–167, 1997. Special issue on time integration (Amsterdam, 1996).

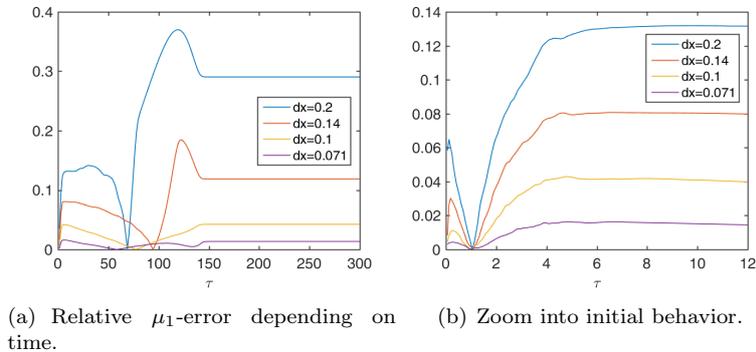[2] J. Bec and K. Khanin. Burgers turbulence. *Phys. Rep.*, 447(1-2):1–66, 2007.

(a) Relative μ_1-error depending on time.

(b) Zoom into initial behavior.

FIGURE 7. The relative error $\frac{|\mu_{1,\mathrm{ref}}(\tau)-\mu_1(\tau)|}{|\mu_{1,\mathrm{ref}}(\tau)|}$ of the algebraic variable corresponding to the speed of the scaling μ_1 for different step-sizes $\Delta\xi_1 = \Delta\xi_2 = dx$ drawn as a function of time.

[3] W.-J. Beyn, D. Otten, and J. Rottmann-Matthes. Stability and computation of dynamic patterns in PDEs. In *Current challenges in stability issues for numerical differential equations. Lectures of the CIME-EMS summer school, Cetraro, Italy, June 2011*, pages 89–172. Cham: Springer; Firenze: Fondazione CIME, 2014.

[4] W.-J. Beyn, D. Otten, and J. Rottmann-Matthes. Computation and Stability of Traveling Waves in Second Order Evolution Equations. Preprint 2016/15, CRC 1173, Karlsruhe Institute of Technology, 2016.

[5] W.-J. Beyn and V. Thümmler. Freezing solutions of equivariant evolution equations. *SIAM J. Appl. Dyn. Syst.*, 3(2):85–116 (electronic), 2004.

[6] J. M. Burgers. A mathematical model illustrating the theory of turbulence. *Advances in Applied Mechanics*, 1948.

[7] E. Hairer, C. Lubich, and M. Roche. The numerical solution of differential-algebraic systems by Runge-Kutta methods. Lecture Notes in Mathematics, 1409. Berlin etc.: Springer-Verlag. vii, 139 p. DM 25.00 (1989)., 1989.

[8] E. Hairer and G. Wanner. *Solving ordinary differential equations. II: Stiff and differential-algebraic problems. 2nd rev. ed.* Berlin: Springer, 2nd rev. ed. edition, 1996.

[9] C. Hu and C.-W. Shu. Weighted essentially non-oscillatory schemes on triangular meshes. *J. Comput. Phys.*, 150(1):97–127, 1999.

[10] A. Kurganov and E. Tadmor. New high-resolution central schemes for nonlinear conservation laws and convection-diffusion equations. *J. Comput. Phys.*, 160(1):241–282, 2000.

[11] W. S. Martinson and P. I. Barton. A differentiation index for partial differential-algebraic equations. *SIAM J. Sci. Comput.*, 21(6):2295–2315, 2000.

[12] J. Rottmann-Matthes. Stability and Freezing of Nonlinear Waves in First Order Hyperbolic PDEs. *J. Dynam. Differential Equations*, 24(2):341–367, 2012.

[13] J. Rottmann-Matthes. Stability and freezing of waves in non-linear hyperbolic-parabolic systems. *IMA J. Appl. Math.*, 77(3):420–429, 2012.

[14] J. Rottmann-Matthes. Freezing similarity solutions in multi-dimensional Burgers' Equation. Preprint 2016/27, CRC 1173, Karlsruhe Institute of Technology, 2016.

[15] C. W. Rowley, I. G. Kevrekidis, J. E. Marsden, and K. Lust. Reduction and reconstruction for self-similar dynamical systems. *Nonlinearity*, 16(4):1257–1275, 2003.

[16] C.-W. Shu. Total-variation-diminishing time discretizations. *SIAM J. Sci. Statist. Comput.*, 9(6):1073–1084, 1988.

[17] C.-W. Shu and S. Osher. Efficient implementation of essentially nonoscillatory shock-capturing schemes. *J. Comput. Phys.*, 77(2):439–471, 1988.

[18] V. Thümmler. The effect of freezing and discretization to the asymptotic stability of relative equilibria. *J. Dynam. Differential Equations*, 20(2):425–477, 2008.

APPENDIX A. DISCRETIZATION OF THE HYPERBOLIC PART

For the discretization of the hyperbolic part in (20a), we briefly review and adapt a scheme introduced by Kurganov and Tadmor in [10] (KT-scheme). In particular, we need an adaptation for non-homogeneous

flux functions, i.e. the case of hyperbolic conservation laws of the form

$$u_\tau + \frac{d}{d\xi} f(\xi, u) = 0.$$

In this appendix u may be $\mathbb{R}^m$ valued, but in the actual application in Section 3 it is always a scalar. For the KT-scheme, a uniform grid $\xi_j = \xi_0 + j\Delta\xi$, $j \in \mathbb{Z}$ in $\mathbb{R}$ is chosen and one assumes that at a time instance τ^n an approximation of the average mass of the function u in the spatial cells $(\xi_{j-\frac{1}{2}}, \xi_{j+\frac{1}{2}})$, $\xi_{j\pm\frac{1}{2}} = \xi_j \pm \frac{\Delta\xi}{2}$ $j \in \mathbb{Z}$, is given as $u_j^n \in \mathbb{R}^m$. I.e. $u_j^n \approx \frac{1}{\Delta\xi} \int_{\xi_{j-\frac{1}{2}}}^{\xi_{j+\frac{1}{2}}} u(\xi, t^n)\, d\xi$. From this grid function one obtains the piecewise linear reconstruction at the time instance τ^n as

$$\widetilde{u}(\xi, t^n) = \sum_j \left(u_j^n \mathbb{1}_{[\xi_{j-\frac{1}{2}}, \xi_{j+\frac{1}{2}})}(\xi) + (u_\xi)_j^n (\xi - \xi_j) \mathbb{1}_{[\xi_{j-\frac{1}{2}}, \xi_{j+\frac{1}{2}})}(\xi) \right),$$

where $(u_\xi)_j^n$ is a suitable choice of the slope of this piecewise linear function in the cell $(\xi_{j-\frac{1}{2}}, \xi_{j+\frac{1}{2}})$. These "suitable" slopes are given by the "minmod"-reconstruction, i.e. for a fixed $\theta \in [1, 2]$ the slopes are given as

$$(u_\xi)_j^n = \mathrm{mm} \left(\theta \frac{u_j - u_{j-1}}{\Delta\xi}, \frac{u_{j+1} - u_{j-1}}{2\Delta\xi}, \theta \frac{u_{j+1} - u_j}{\Delta\xi} \right),$$

where

(70) $$\mathrm{mm}(a_1, \ldots, a_k) = \max\Big(\min(a_1, 0), \ldots, \min(a_k, 0)\Big) + \min\Big(\max(a_1, 0), \ldots, \max(a_k, 0)\Big).$$

In the vector-valued case (70) is understood in the component wise sense. The idea of the KT-scheme is to use an artificial finer grid, which depends on the time step size $\Delta\tau$ and separates the smooth and non-smooth regions of the solution. In the original paper [10], local (maximal) wave speeds are calculated and a spatial grid based on these is chosen. Since we ultimately intend to apply the scheme to the PDAE-system (20), for which the wave speeds nonlinearly depend on the solution, we choose a sufficiently large $a > 0$, which bounds the spectral radius of $\frac{\partial}{\partial u} f(\xi, u)$. Note that this is obviously not possible for $f(\xi, u) = \xi u$, $\xi \in \mathbb{R}$, but because we will restrict to compact domains in the end, we assume that the spectral radius is uniformly bounded in ξ for bounded u.
The new grid is then given by

$$\ldots < \xi_{j-1} < \xi_{j-\frac{1}{2}, l} = \xi_{j-\frac{1}{2}} - a\Delta\tau < \xi_{j-\frac{1}{2}, r} = \xi_{j-\frac{1}{2}} + a\Delta\tau < \xi_j < \ldots$$

for $\Delta\tau$ sufficiently small. We remark that for $\Delta\tau \searrow 0$, the new grid points $\xi_{j-\frac{1}{2}, l}$ and $\xi_{j-\frac{1}{2}, r}$ both converge to $\xi_{j-\frac{1}{2}}$, the first from the left and the second from the right. The principal idea now is, to
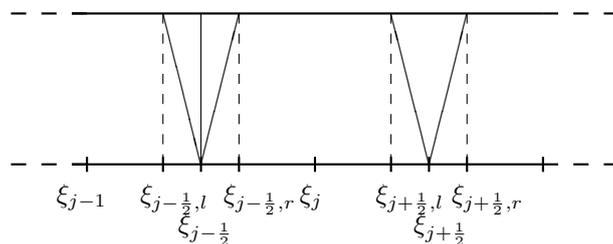

FIGURE 8. Sketch of the grid and smooth and non-smooth parts of the solution.

use the integral form of the conservation law in the smooth and non-smooth regions for the calculation of the mass at the new time instance τ^{n+1}. We begin with the non-smooth part:

$$\frac{1}{\Delta\xi_{\frac{1}{2}}} \int_{\xi_{j-\frac{1}{2},l}}^{\xi_{j-\frac{1}{2},r}} u(\xi, \tau^{n+1})\, d\xi = \frac{1}{2a\Delta\tau} \Big(\int_{\xi_{j-\frac{1}{2},l}}^{\xi_{j-\frac{1}{2},r}} \widetilde{u}(\xi, \tau^n)\, d\xi$$

$$- \int_{\tau^n}^{\tau^{n+1}} f\big(\xi_{j-\frac{1}{2},r}, u(\xi_{j-\frac{1}{2},r}, \tau)\big)\, d\tau + \int_{\tau^n}^{\tau^{n+1}} f\big(\xi_{j-\frac{1}{2},l}, u(\xi_{j-\frac{1}{2},l}, \tau)\big)\, d\tau \Big),$$

where $\Delta\xi_{\frac{1}{2}} = 2a\Delta\tau = \xi_{j-\frac{1}{2},r} - \xi_{j-\frac{1}{2},l}$. The time integrals are in the smooth regions of the solution (the dashed vertical lines in Figure 8). We approximate them by the midpoint rule, so that we need the value of the solution u at $\xi_{j-\frac{1}{2},l}$, $\xi_{j-\frac{1}{2},r}$ and time instance $\tau^n + \frac{\Delta\tau}{2}$. In a smooth region this value of u is approximately

$$u(\xi_{j-\frac{1}{2},l}, \tau^{n+\frac{1}{2}}) \approx u_{j-\frac{1}{2},l}^n - \frac{\Delta\tau}{2} \left(\tfrac{\partial}{\partial\xi} f(\xi_{j-\frac{1}{2},l}, u_{j-\frac{1}{2},l}^n) + \tfrac{\partial}{\partial u} f(\xi_{j-\frac{1}{2},l}, u_{j-\frac{1}{2},l}^n)(u_\xi)_j^n \right)$$

$$:= u_{j-\frac{1}{2},l}^{n+\frac{1}{2}}$$

and the same for l replaced by r. For the average value of the solution u at the new time instance τ^{n+1} in the spatial interval $(\xi_{j-\frac{1}{2},l}, \xi_{j+\frac{1}{2},r})$ this yields the approximation

$$
\begin{aligned}
w_{j-\frac{1}{2}}^{n+1} &:= \frac{u_{j-1}^n + u_j^n}{2} + \frac{\Delta\xi - a\Delta t}{4}\big((u_\xi)_{j-1}^n - (u_\xi)_j^n\big) - \frac{1}{2a}\big(f(\xi_{j-\frac{1}{2},r}, u_{j-\frac{1}{2},r}^{n+\frac{1}{2}}) - f(\xi_{j-\frac{1}{2},l}, u_{j-\frac{1}{2},l}^{n+\frac{1}{2}})\big) \\
&\approx \frac{1}{\Delta\xi_{\frac{1}{2}}} \int_{\xi_{j-\frac{1}{2},l}}^{\xi_{j-\frac{1}{2},r}} u(\xi, t^{n+1})\, d\xi.
\end{aligned}
$$

(71)

Similarly, the average of the solution at the new time instance τ^{n+1} in the spatial interval $(\xi_{j-\frac{1}{2},r}, \xi_{j+\frac{1}{2},l})$ is approximated by

$$
\begin{aligned}
w_j^{n+1} &:= u_j^n - \frac{\Delta\tau}{\Delta\xi - 2a\Delta\tau}\big(f(\xi_{j+\frac{1}{2},l}, u_{j+\frac{1}{2},l}^{n+\frac{1}{2}}) - f(\xi_{j-\frac{1}{2},r}, u_{j-\frac{1}{2},r}^{n+\frac{1}{2}})\big) \\
&\approx \frac{1}{\Delta\xi - \Delta\xi_{\frac{1}{2}}} \int_{\xi_{j-\frac{1}{2},r}}^{\xi_{j+\frac{1}{2},l}} u(\xi, t^{n+1})\, d\xi.
\end{aligned}
$$

(72)

To come back from the new grid back to the original one, a piecewise linear reconstruction $\widetilde{w}$ of the grid function w^{n+1} is calculated and then u_j^{n+1} is obtained by integration over the cells $(\xi_{j-\frac{1}{2}}, \xi_{j+\frac{1}{2}})$. Finally, one obtains the fully discrete scheme:

$$
\begin{aligned}
u_j^{n+1} = \frac{1}{\Delta\xi} \Big[&(\xi_{j-\frac{1}{2},r} - \xi_{j-\frac{1}{2}})w_{j-\frac{1}{2}}^{n+1} + (w_\xi)_{j-\frac{1}{2}}^{n+1} \frac{(\xi_{j-\frac{1}{2},r} - \xi_{j-\frac{1}{2}})^2}{2} \\
&+ (\xi_{j+\frac{1}{2},l} - \xi_{j-\frac{1}{2},r})w_j^{n+1} \\
&+ (\xi_{j+\frac{1}{2}} - \xi_{j+\frac{1}{2},l})w_{j+\frac{1}{2}}^{n+1} - (w_\xi)_{j+\frac{1}{2}}^{n+1} \frac{(\xi_{j+\frac{1}{2}} - \xi_{j+\frac{1}{2},l})^2}{2} \Big],
\end{aligned}
$$

(73)

where $w_{j\pm\frac{1}{2}}^{n+1}$ and w_j^{n+1} are given by (71) and (72) and

$$(w_\xi)_{j-\frac{1}{2}}^{n+1} = \frac{2}{\Delta\xi} \operatorname{mm}\big(w_j^{n+1} - w_{j-\frac{1}{2}}^{n+1}, w_{j-\frac{1}{2}}^{n+1} - w_{j-1}^{n+1}\big).$$

The fully discrete scheme (73) admits a semi-discrete version, i.e. a method of lines system, which we will use in our discretization of (20). To see this, let $\lambda = \Delta\tau/\Delta\xi$, in which we consider $\Delta\xi$ as a fixed quantity and are interested in the limit $\Delta\tau \to 0$ so that $\mathcal{O}(\lambda^2) = \mathcal{O}(\Delta\tau^2)$. We note, that the summands in (73) can be written in the following form, where we use $\xi_{j-\frac{1}{2}} - \xi_{j-\frac{1}{2},l} = \xi_{j-\frac{1}{2},r} - \xi_{j-\frac{1}{2}} = a\Delta\tau$:

(74) $$(\xi_{j-\frac{1}{2},r} - \xi_{j-\frac{1}{2}})w_{j-\frac{1}{2}}^{n+1} = \frac{a\Delta\tau}{2}\big(u_{j-1}^n + \frac{\Delta\xi}{2}(u_\xi)_{j-1}^n + u_j^n - \frac{\Delta\xi}{2}(u_\xi)_j^n\big)$$

$$- \frac{\Delta\tau}{2}\big(f(\xi_{j-\frac{1}{2},r}, u_{j-\frac{1}{2},r}^{n+\frac{1}{2}}) - f(\xi_{j-\frac{1}{2},l}, u_{j-\frac{1}{2},l}^{n+\frac{1}{2}})\big) + \mathcal{O}(\lambda^2),$$

$$(75) \qquad (w_\xi)_{j-\frac{1}{2}}^{n+1} \frac{(\xi_{j-\frac{1}{2},r} - \xi_{j-\frac{1}{2}})^2}{2} = \mathcal{O}(\lambda^2)$$

$$(76) \qquad (\xi_{j+\frac{1}{2},l} - \xi_{j-\frac{1}{2},r}) w_j^{n+1} = \Delta\xi u_j^n - 2a\Delta\tau u_j^n - \Delta\tau\big(f(\xi_{j+\frac{1}{2},l}, u_{j+\frac{1}{2},l}^{n+\frac{1}{2}}) - f(\xi_{j-\frac{1}{2},r}, u_{j-\frac{1}{2},r}^{n+\frac{1}{2}})\big),$$

$$(77) \qquad (\xi_{j+\frac{1}{2}} - \xi_{j+\frac{1}{2},l}) w_{j+\frac{1}{2}}^{n+1} = \frac{a\Delta\tau}{2}\big(u_j^n + \frac{\Delta\xi}{2}(u_\xi)_j^n + u_{j+1}^n - \frac{\Delta\xi}{2}(u_\xi)_{j+1}^n\big)$$
$$- \frac{\Delta\tau}{2}\big(f(\xi_{j+\frac{1}{2},r}, u_{j+\frac{1}{2},r}^{n+\frac{1}{2}}) - f(\xi_{j+\frac{1}{2},l}, u_{j+\frac{1}{2},l}^{n+\frac{1}{2}})\big) + \mathcal{O}(\lambda^2),$$

$$(78) \qquad (w_\xi)_{j+\frac{1}{2}}^{n+1} \frac{(\xi_{j+\frac{1}{2}} - \xi_{j+\frac{1}{2},l})^2}{2} = \mathcal{O}(\lambda^2).$$

The semi-discrete version is then obtained by subtracting u_j^n from both sides of (73), dividing by $\Delta\tau$ and considering the limit $\Delta\tau \to 0$. Using (74)–(78) and the convergences $\xi_{j\pm\frac{1}{2},l/r} \to \xi_{j\pm\frac{1}{2}}$, $u_{j-\frac{1}{2},l}^{n+\frac{1}{2}} \to u_{j-\frac{1}{2}}^{n,-} = u_{j-1}^n + \frac{\Delta\xi}{2}(u_\xi)_{j-1}^n$, and $u_{j-\frac{1}{2},r}^{n+\frac{1}{2}} \to u_{j-\frac{1}{2}}^{n,+} = u_j^n - \frac{\Delta\xi}{2}(u_\xi)_j^n$ as $\Delta\tau \to 0$, the continuity properties of f imply that the limit of the difference quotient exists. The final result is the following semi-discrete scheme (method of lines system):

$$(79) \qquad \frac{d}{d\tau} u_j = \frac{1}{2\Delta\xi}\Big(\big(f(\xi_{j-\frac{1}{2}}, u_{j-\frac{1}{2}}^-) + f(\xi_{j-\frac{1}{2}}, u_{j-\frac{1}{2}}^+)\big) - \big(f(\xi_{j+\frac{1}{2}}, u_{j+\frac{1}{2}}^-) + f(\xi_{j+\frac{1}{2}}, u_{j+\frac{1}{2}}^+)\big)\Big)$$
$$+ \frac{a}{2\Delta\xi}\big(u_{j-\frac{1}{2}}^- - u_{j-\frac{1}{2}}^+ - u_{j+\frac{1}{2}}^- + u_{j+\frac{1}{2}}^+\big), \quad j \in \mathbb{Z},$$

where

$$(80) \qquad u_{j-\frac{1}{2}}^- = u_{j-1} + \frac{1}{2}\,\mathrm{mm}\big(\theta(u_{j-1} - u_{j-2}), \frac{u_j - u_{j-2}}{2}, \theta(u_j - u_{j-1})\big),$$
$$u_{j-\frac{1}{2}}^+ = u_j - \frac{1}{2}\,\mathrm{mm}\big(\theta(u_j - u_{j-1}), \frac{u_{j+1} - u_{j-1}}{2}, \theta(u_{j+1} - u_j)\big).$$

Before we continue, we state some simple remarks:

Remark A.1.   (1) In the case $f(\xi, u) = f(u)$, (79) reduces to the semi-discrete version of the KT-scheme from [10].
  (2) In the case of a piecewise constant reconstruction of u, the last summand in (79) reduces to $\frac{a}{2\Delta\xi}(u_{j-1} - 2u_j + u_{j+1})$, and can be interpreted as artificial viscosity, that vanishes as $\Delta\xi \to 0$.
  (3) The flux function f enters linearly into the semi-discrete scheme, this is an important observation, because it allows us to derive a method of lines system for the PDE-part of the PDAE (20), without knowing the algebraic variables μ in advance. To the resulting system we may apply a so called half-explicit scheme for the PDAE (see [7])
  (4) The method of lines system (79) can be written in conservative form as

$$u_j' = -\frac{H_{j+\frac{1}{2}} - H_{j-\frac{1}{2}}}{\Delta\xi},$$

where

$$H_{j+\frac{1}{2}} = \frac{f(\xi_{j+\frac{1}{2}}, u_{j+\frac{1}{2}}^+) + f(\xi_{j+\frac{1}{2}}, u_{j+\frac{1}{2}}^-)}{2} - a\big(u_{j+\frac{1}{2}}^+ - u_{j+\frac{1}{2}}^-\big).$$

Multi-dimensional version
There is no difficulty in performing the same calculation in the multi-dimensional setting. We only

present the result for the 2-dimensional case: For this we consider a system of hyperbolic conservation laws of the form

$$u_\tau + \frac{d}{d\xi} f(\xi, \eta, u) + \frac{d}{d\eta} g(\xi, \eta, u) = 0.$$

Choose a uniform spatial grid $(\xi_j, \eta_k) = (\xi_0 + j\Delta\xi, \eta_0 + k\Delta\eta)$ and assume that a grid function $(u_{j,k})$ is given on this grid, where $u_{j,k}(\tau)$ denotes the average mass in the cell $(\xi_{j-\frac{1}{2}}, \xi_{j+\frac{1}{2}}) \times (\eta_{k-\frac{1}{2}}, \eta_{k+\frac{1}{2}})$, $\xi_{j\pm\frac{1}{2}} = \xi_j \pm \frac{\Delta\xi}{2}$ and similarly $\eta_{k\pm\frac{1}{2}} = \eta_k \pm \frac{\Delta\eta}{2}$ at time τ. Adapting the above derivation, we obtain the following 2-dimensional version of the semi-discrete KT-scheme:

(81)
$$
\begin{aligned}
u'_{j,k} = &\frac{1}{2\Delta\xi}\Big[\big(f(\xi_{j-\frac{1}{2}}, \eta_k, u^-_{j-\frac{1}{2},k}) + f(\xi_{j-\frac{1}{2}}, \eta_k, u^+_{j-\frac{1}{2},k})\big) - \big(f(\xi_{j+\frac{1}{2}}, \eta_k, u^-_{j+\frac{1}{2},k}) + f(\xi_{j+\frac{1}{2}}, \eta_k, u^+_{j+\frac{1}{2},k})\big)\Big] \\
&+ \frac{1}{2\Delta\eta}\Big[\big(g(\xi_j, \eta_{k-\frac{1}{2}}, u^-_{j,k-\frac{1}{2}}) + g(\xi_j, \eta_{k-\frac{1}{2}}, u^+_{j,k-\frac{1}{2}})\big) - \big(g(\xi_j, \eta_{k+\frac{1}{2}}, u^-_{j,k+\frac{1}{2}}) + g(\xi_j, \eta_{k+\frac{1}{2}}, u^+_{j,k+\frac{1}{2}})\big)\Big] \\
&+ \frac{a}{2\Delta\xi}\Big(u^-_{j-\frac{1}{2},k} - u^+_{j-\frac{1}{2},k} - u^-_{j+\frac{1}{2},k} + u^+_{j+\frac{1}{2},k}\Big) \\
&+ \frac{a}{2\Delta\eta}\Big(u^-_{j,k-\frac{1}{2}} - u^+_{j,k-\frac{1}{2}} - u^-_{j,k+\frac{1}{2}} + u^+_{j,k+\frac{1}{2}}\Big).
\end{aligned}
$$

In (81) the number a is again assumed to be an upper bound for the maximum of the spectral radii of $\frac{\partial}{\partial u} f(\xi, \eta, u)$ and $\frac{\partial}{\partial u} g(\xi, \eta, u)$ for all relevant ξ, η, u. We assume that such an upper bound exists. The one-sided limits appearing in (81) are given by

(82)
$$
\begin{aligned}
u^-_{j-\frac{1}{2},k} &= u_{j-1,k} + \tfrac{1}{2} \text{mm}\big(\theta(u_{j-1,k} - u_{j-2,k}), \frac{u_{j,k} - u_{j-2,k}}{2}, \theta(u_{j,k} - u_{j-1,k})\big), \\
u^+_{j-\frac{1}{2},k} &= u_{j,k} - \tfrac{1}{2} \text{mm}\big(\theta(u_{j,k} - u_{j-1,k}), \frac{u_{j+1,k} - u_{j-1,k}}{2}, \theta(u_{j+1,k} - u_{j,k})\big), \\
u^-_{j,k-\frac{1}{2}} &= u_{j,k-1} + \tfrac{1}{2} \text{mm}\big(\theta(u_{j,k-1} - u_{j,k-2}), \frac{u_{j,k} - u_{j,k-2}}{2}, \theta(u_{j,k} - u_{j,k-1})\big), \\
u^+_{j,k-\frac{1}{2}} &= u_{j,k} - \tfrac{1}{2} \text{mm}\big(\theta(u_{j,k} - u_{j,k-1}), \frac{u_{j,k+1} - u_{j,k-1}}{2}, \theta(u_{j,k+1} - u_{j,k})\big).
\end{aligned}
$$